0830-L-02 NAS1.29/3-2:00-04

NASA Tech Briefs

National Aeronautics and
Space Administration

Electronic Components and Circuits

Electronic Systems

Physical Sciences

Materials

Computer Programs

Mechanics

Machinery

Bar
2002 004138

Fabrication Technology

Mathematics and Information Sciences

Life Sciences

INTRODUCTION

Tech Briefs are short announcements of innovations originating from research and development activities of the National Aeronautics and Space Administration. They emphasize information considered likely to be transferable across industrial, regional, or disciplinary lines and are issued to encourage commercial application.

Availability of NASA Tech Briefs and TSPs

Requests for individual Tech Briefs or for Technical Support Packages (TSPs) announced herein should be addressed to

National Technology Transfer Center
Telephone No. **(800) 678-6882** or via World Wide Web at **www2.nttc.edu/leads/**

Please reference the control numbers appearing at the end of each Tech Brief. Information on NASA's Commercial Technology Team, its documents, and services is also available at the same facility or on the World Wide Web at **www.nctn.hq.nasa.gov**.

Commercial Technology Offices and Patent Counsels are located at NASA field centers to provide technology-transfer access to industrial users. Inquiries can be made by contacting NASA field centers and program offices listed below.

NASA Field Centers and Program Offices

Ames Research Center
Carolina Blake
(650) 604-0893 or
cblake@mail.arc.nasa.gov

Dryden Flight Research Center
Lee Duke
(805) 258-3802 or
lee.duke@dfrc.nasa.gov

Goddard Space Flight Center
George Alcorn
(301) 286-5810 or
galcorn@gsfc.nasa.gov

Jet Propulsion Laboratory
Merle McKenzie
(818) 354-2577 or
merle.mckenzie@commail.jpl.nasa.gov

Johnson Space Center
Hank Davis
(281) 483-0474 or
hdavis@gp101.jsc.nasa.gov

John F. Kennedy Space Center
Gale Allen
(407) 867-6626 or
gallen-1@ksc.nasa.gov

Langley Research Center
Dr. Joseph S. Heyman
(804) 864-6006 or
j.s.heyman@larc.nasa.gov

Glenn Research Center
Larry Viterna
(216) 433-3484 or
cto@lerc.nasa.gov

George C. Marshall Space Flight Center
Sally Little
(256) 544-4266 or
sally.little@msfc.nasa.gov

John C. Stennis Space Center
Kirk Sharp
(228) 688-1929 or
ksharp@ssc.nasa.gov

NASA Program Offices
At NASA Headquarters there are seven major program offices that develop and oversee technology projects of potential interest to industry:

Carl Ray
Small Business Innovation Research Program (SBIR) & Small Business Technology Transfer Program (STTR)
(202) 358-4652 or
cray@mail.hq.nasa.gov

Dr. Robert Norwood
Office of Aeronautics and Space Transportation Technology (Code R)
(202) 358-2320 or
rnorwood@mail.hq.nasa.gov

John Mulcahy
Office of Space Flight (Code MP)
(202) 358-1401 or
jmulcahy@mail.hq.nasa.gov

Gerald Johnson
Office of Aeronautics (Code R)
(202) 358-4711 or
g_johnson@aeromail.hq.nasa.gov

Bill Smith
Office of Space Science (Code S)
(202) 358-2473 or
wsmith@sm.ms.ossa.hq.nasa.gov

Roger Crouch
Office of Microgravity Science Applications (Code U)
(202) 358-0689 or
rcrouch@hq.nasa.gov

Granville Paules
Office of Mission to Planet Earth (Code Y)
(202) 358-0706 or
gpaules@mtpe.hq.nasa.gov

National Aeronautics and Space Administration

TechBriefs

April 2000
00-04

5	Electronic Components and Circuits	
11	Electronic Systems	
19	Physical Sciences	
25	Materials	
31	Computer Programs	
35	Mechanics	
41	Machinery	
45	Mathematics and Information Sciences	
51	Life Sciences	

This document was prepared under the sponsorship of the National Aeronautics and Space Administration. Neither the United States Government nor any person acting on behalf of the United States Government assumes any liability resulting from the use of the information contained in this document, or warrants that such use will be free from privately owned rights.

4

BLANK PAGE

Electronic Components and Circuits

Hardware, Techniques, and Processes

7 Ultracapacitors Store Energy in a Hybrid Electric Vehicle
8 Controller for Bistable Brakes
9 Dual-Tuning Microwave Phase Shifter

BLANK PAGE

Ultracapacitors Store Energy in a Hybrid Electric Vehicle

Capacitors are superior to batteries with respect to energy density, longevity, and performance.

John H. Glenn Research Center, Cleveland, Ohio

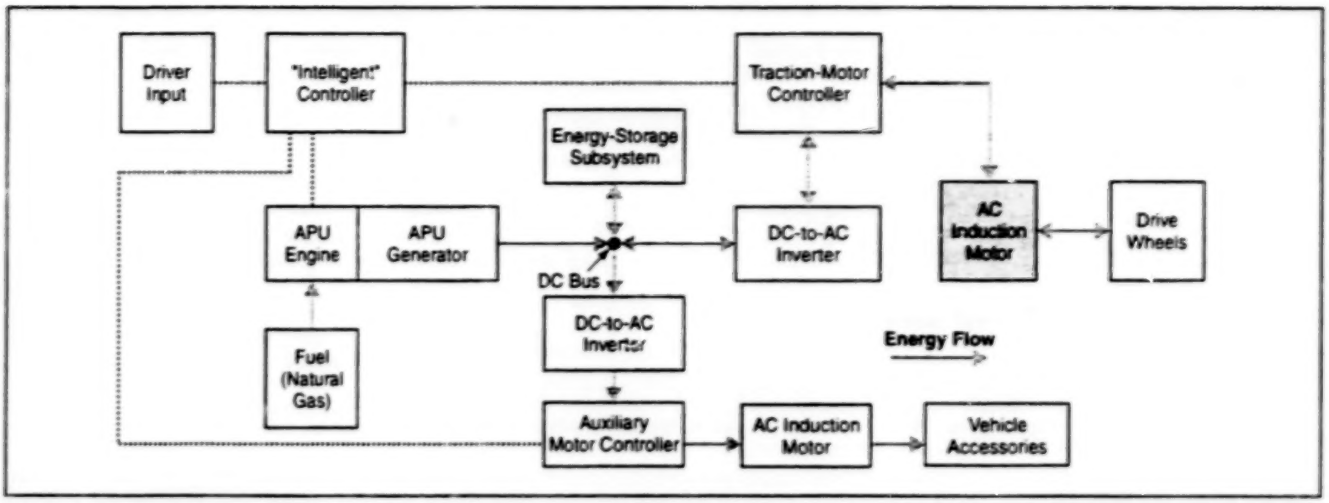

Figure 1. The **HETB Power System** includes a dedicated power-management controller and an energy-storage subsystem that utilizes capacitors instead of batteries.

A government/industry/academic cooperative has developed a hybrid electric transit bus (HETB). The goals of the development program, which continues, include doubling the fuel economy of city transit buses currently in service, and reducing emissions to one-tenth of the levels allowed by Environmental Protection Agency (EFA) standards. A unique aspect of the power system of the HETB is the use of capacitors in its the energy-storage subsystem. At a gross weight of more than 17,000 kg, this is the largest known vehicle to use capacitors to store energy.

Energy storage has always been a problem for electric vehicles, and even a greater problem for hybrid electric vehicles. In a purely electric vehicle, energy is stored, usually in batteries, and then used to power the vehicle until the energy is depleted. At that time energy is stored once more by recharging the batteries. In a hybrid electric vehicle, energy is constantly being stored and used; the repeated charging and discharging puts a tremendous strain on the batteries. This type of use reduces the lifetimes of presently available batteries.

Ultracapacitors that are now available eliminate many of the problems of batteries for hybrid electric vehicles. The ultracapacitors used in the HETB are electrochemical capacitors, which have extremely high volumetric capacitances because of large electrode surface areas and very small electrode separations. The cycle lives of capacitors can

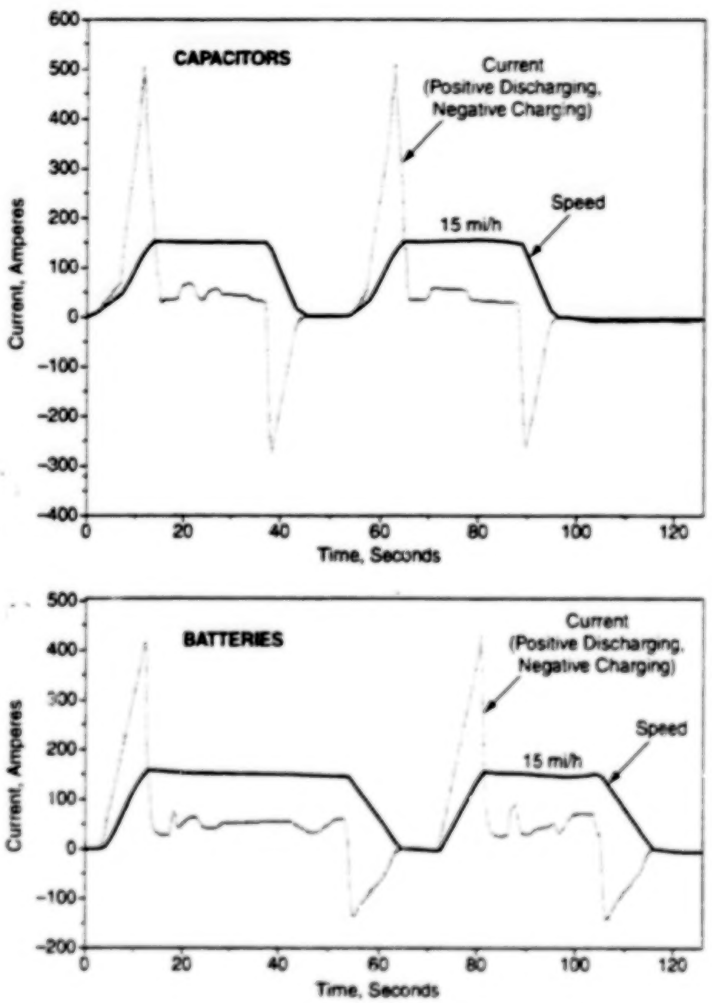

Figure 2. **Charging and Discharging Currents** were measured in two tests, in each of which the HETB was driven through two cycles at speeds between 0 and 15 mi/h (0 and 24 km/h). In one test, capacitors were used to store energy; in the other test, batteries were used.

be extremely long relative to those of batteries. Thus, it may never be necessary to replace the energy-storage medium in the HETB; consequently, the reliability of the HETB energy system is greater than it would be if batteries were used, the life-of-system cost is reduced, and adverse environmental effects are diminished.

Capacitors can also function at power densities greater than those of batteries. Therefore, very high power levels can be provided during acceleration and can be absorbed during charging. Capacitors have excellent low-temperature characteristics, do not require maintenance, and provide consistent performance over time. In addition, capacitors promote safety in electric vehicles because of their relative ease of discharge.

Figure 1 is a block diagram of the HETB power system. A dedicated power-management controller has been developed to coordinate the operation of all of the various vehicle components. The auxiliary power unit (APU) is set to provide the normal average power level required by the vehicle. Power surges such as those needed for acceleration and climbing hills are provided by a combination of the APU and the ultracapacitors.

Regenerative braking is also provided on the vehicle. Regenerative braking takes advantage of energy available from the traction drive system during braking to charge the energy-storage system. Because of their higher power-density limits and their greater efficiency in capturing energy, capacitors can take much greater advantage of regenerative braking than do batteries. The plots in Figure 2 show the superiority of capacitors over batteries as sources of current for the traction motor during acceleration and as acceptors of braking current during deceleration.

This work was done by Jeffrey C. Brown, Dennis J. Eichenberg, William K. Thompson, and Larry A. Viterna of **Glenn Research Center** *and Richard F. Soltis of Cortez III. Further information is contained in a TSP [see page 1].*

Inquiries concerning rights for the commercial use of this invention should be addressed to NASA Glenn Research Center, Commercial Technology Office, Attn: Steve Fedor, Mail Stop 4–8, 21000 Brookpark Road, Cleveland, Ohio 44135. Refer to LEW-16876.

Controller for Bistable Brakes

This circuit generates pulses for switching brakes on and off.

John H. Glenn Research Center, Cleveland, Ohio

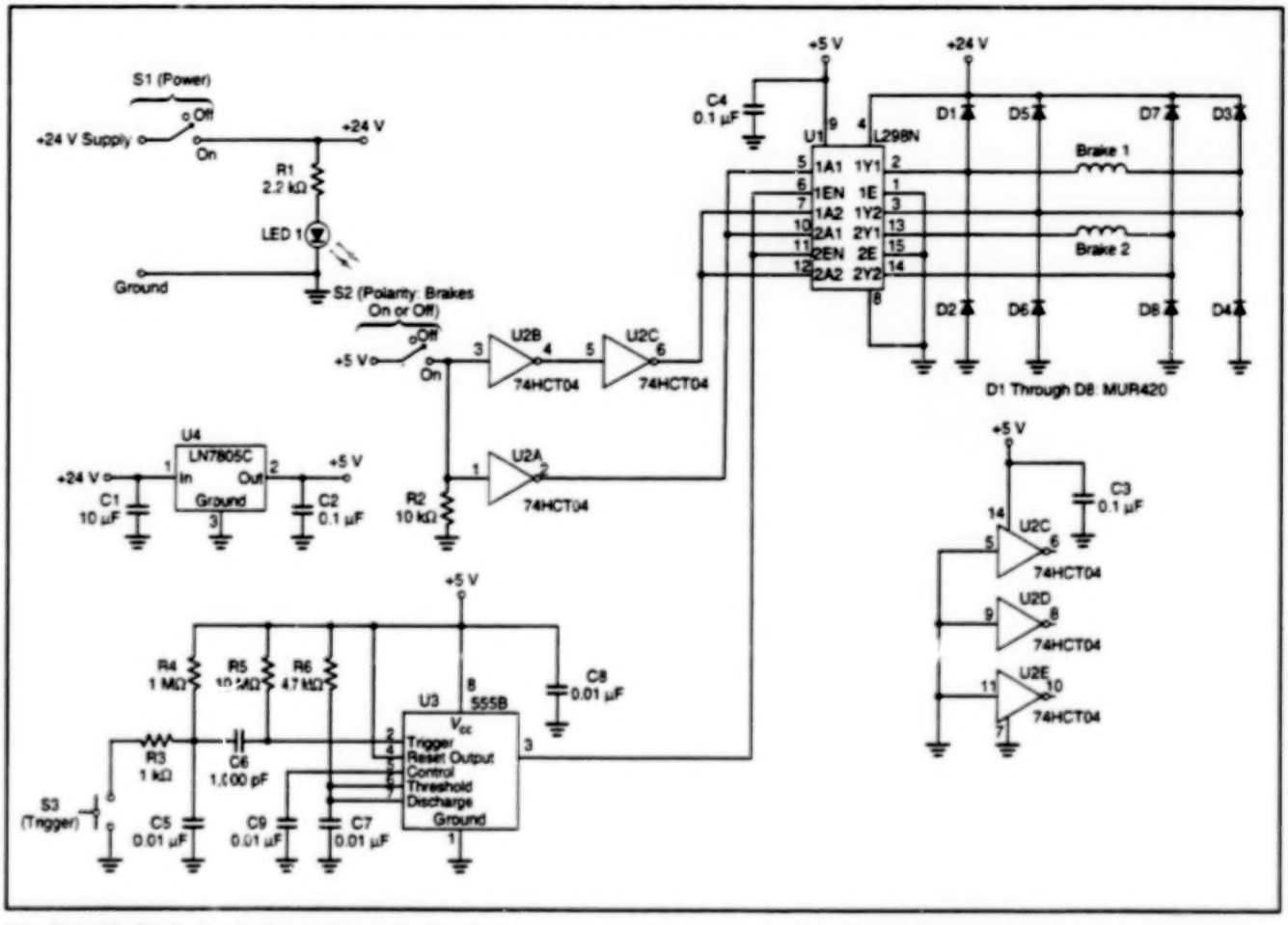

This **Bistable-Brake Controller** sends pulses of current to brakes 1 and 2 when switch S3 is closed. The polarity of the pulses is selected by closing or opening S2.

The circuit shown in the figure is a controller for bistable brakes. The use of bistable brakes reduces energy consumption and spurious heating, as explained below.

A bistable brake is one that can stay in the "on" or "off" position without consuming energy from an outside source. To switch a bistable brake from "on" to "off" or vice versa, all that is needed is a pulse of direct current with a duration of the order of 100 milliseconds. Because no power is consumed except during switching pulses, the energy consumed and the heat dissipated are much less than in the case of an ordinary electromagnetic brake.

In one application, the brakes are parts of a robot to be used in the assembly of the International Space Station. The robot contains 34 joints, each containing and actuated by a small motor/brake unit. Bistable brakes were chosen for these joints because 34 ordinary electromagnetic brakes would consume too much energy. In another application, a bistable brake is part of a droplet-deployment servo system in a droplet-combustion flight experiment; the use of the bistable brake in this system minimizes heat gain by fuel droplets.

The present circuit was developed to make the best use of bistable brakes. This circuit can exert simultaneous control over two bistable brakes, each rated at a potential of 24 V and current of 2 A. The heart of the circuit is U1 — the L298N full-bridge driver. This is a high-voltage, high-current driver designed to accept standard transistor/transistor-logic (TTL) potentials and drive inductive loads. U1 is configured to provide either a positive or a negative pulse of 500-millisecond duration when activated. Switch S2 is used to set the desired polarity through hex inverter U2, which generates the corresponding required inputs for U1. Diodes D1 through D8 serve as clamps to protect U1 against voltage spikes.

Timer U3 is configured as a monostable multivibrator to generate a clean 500-millisecond input pulse for U1 whenever switch S3 is closed. Even if switch S3 is closed for a longer time, the pulse is still no more than 500 milliseconds long; this feature helps to minimize consumption of energy.

Voltage regulator U4 generates the 5-V logic potential from the 24-V power-supply potential. The connection to the power supply is controlled by switch S1.

In operation under manual control, switch S1 is turned on first. Then switch S2 is set to obtain the polarity for turning the brakes on or off as desired. Finally, at the desired moment, switch S3 is closed to command the generation of the pulses to switch the brakes on or off. The circuit can also be adapted to operation under control by a microprocessor.

This work was done by Dennis Eichenberg and John Kolacz of **Glenn Research Center**. *No further documentation is available.*

Inquiries concerning rights for the commercial use of this invention should be addressed to NASA Glenn Research Center, Commercial Technology Office, Attn: Steve Fedor, Mail Stop 4–8, 21000 Brookpark Road, Cleveland, Ohio 44135. Refer to LEW-16818.

Dual-Tuning Microwave Phase Shifter

This device can be tuned electrically, magnetically, or both.

John H. Glenn Research Center, Cleveland, Ohio

A microwave phase shifter that can be tuned by varying both electric and magnetic fields has been developed. This device combines all the advantages of prior electrically and magnetically tunable microwave devices, but in comparison with them, it is smaller and cheaper and it performs better. Devices like this one are suitable for use in monolithic microwave integrated circuits.

This microwave phase shifter is a thin-film ferroelectric/ferrite device. One can alter the propagation of electromagnetic waves in such a device by (1) varying an applied electric field and thereby varying the permittivity of the ferroelectric layer and/or (2) varying an applied magnetic field and thereby varying the permeability of the ferrite layer.

Figure 1 depicts the device as a layered structure and as the main component of a phase-shifting circuit. The substrate is a polycrystalline yttrium iron garnet (YIG) ferrite material. In the fabrication of the device, buffer layers

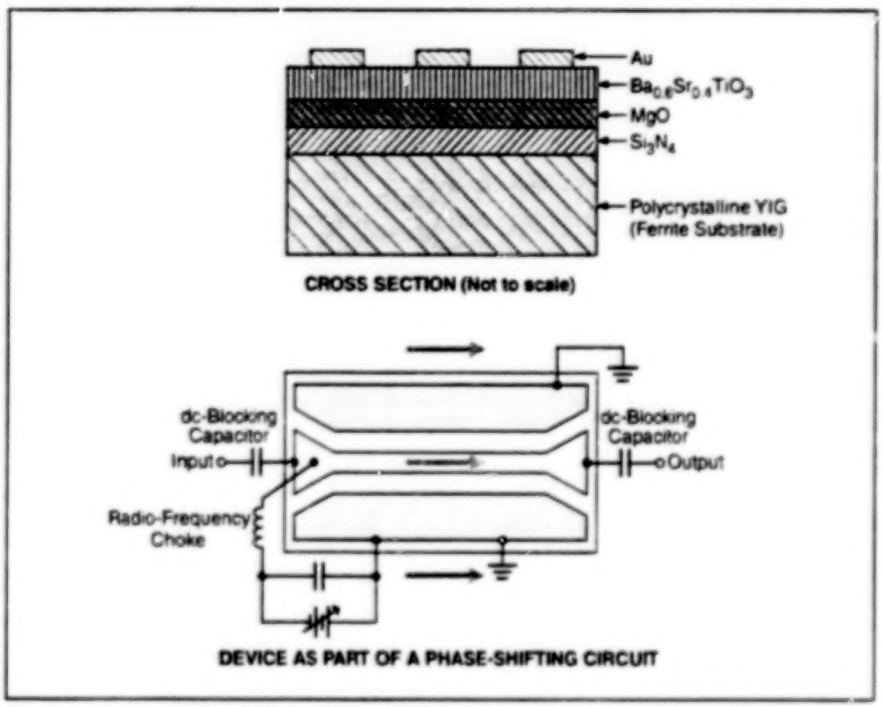

Figure 1. The **Ferroelectric Film and Ferrite Substrate** of this device have electrically variable permittivity and magnetically variable permeability, respectively. These characteristics can be exploited to control the phase shift between the input and output terminals.

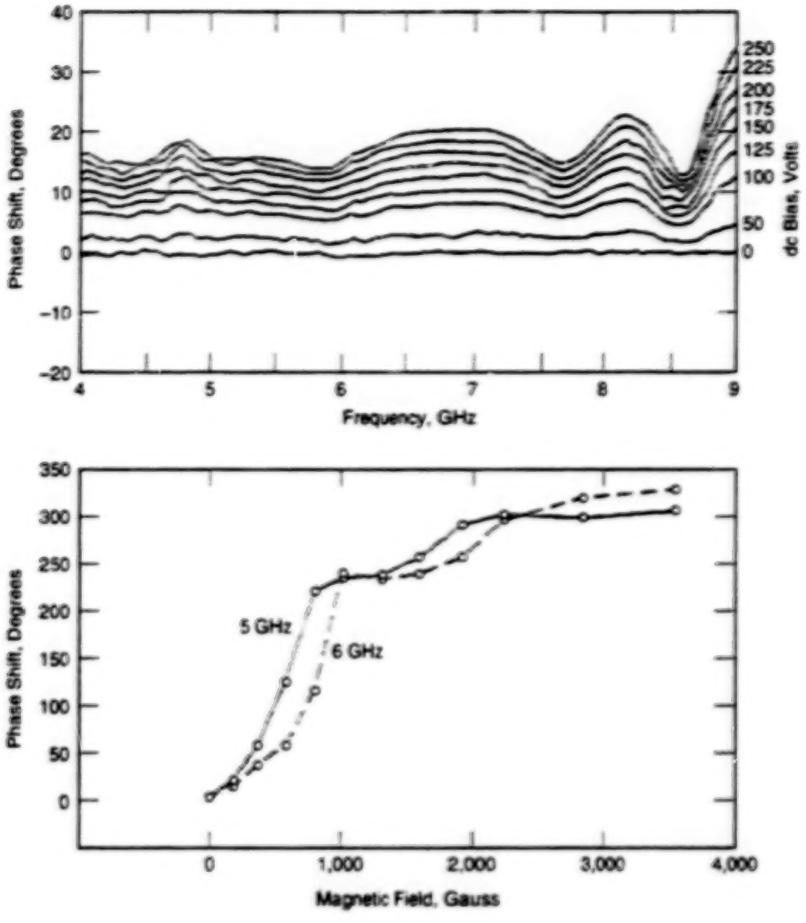

Figure 2. **Phase Shifts** were measured as functions of applied bias voltage (and thus applied electric field), applied magnetic field, and frequency.

of Si_3N_4 and MgO were deposited on the substrate, then the ferroelectric layer was formed by ion-beam-assisted deposition of $Ba_{0.6}Sr_{0.4}TiO_3$ on the MgO. Then a transmission line comprising a central strip and two lateral ground-plane strips was patterned on an electron-beam-evaporated gold film.

In tests of this device, significant phase shift was observed at frequencies up to 18 GHz when an electric bias or a magnetic field was applied. For example (see Figure 2), at a bias of 250 V, phase shifts of 20° and 34° were observed at 7 and 9 GHz, respectively. When an externally generated magnetic field of 800 gauss was applied in tests at 5 and 6 GHz, phase shifts of about 230° were observed. As the magnetic field was increased beyond 800 gauss, the phase shift gradually saturated at about 300°.

This work was done by Hua Jiang of NZ Applied Technologies for **Glenn Research Center**. *Further information is contained in a TSP [see page 1].*

Inquiries concerning rights for the commercial use of this invention should be addressed to NASA Glenn Research Center, Commercial Technology Office, Attn: Steve Fedor, Mail Stop 4–8, 21000 Brookpark Road, Cleveland, Ohio 44135. Refer to LEW-16762.

Electronic Systems

Hardware, Techniques, and Processes

13 High-Rate Modems for Wireless Data Communications
14 Improved HRTF-Based Pseudostereophony
16 Microwave Battery Charger
16 Imaging With a Focal-Plane Array of Ultrasonic Transducers

BLANK PAGE

High-Rate Modems for Wireless Data Communications

Innovative design affords high performance at relatively low cost.

John H. Glenn Research Center, Cleveland, Ohio

A NASA Small Business Innovation Research (SBIR) project has led to the development of high-rate (155.52-Mb/s) modems for use in high-quality wireless data communications. The research was directed toward conceiving innovative signal-processing techniques to reduce costs below those of conventional modems, implementing these techniques in a low-power complementary metal oxide semiconductor (CMOS) application-specific integrated-circuit (ASIC) modulator and a corresponding demodulator, and developing the necessary circuit boards (see figure) and control software. An additional goal of the research was to determine the maximum rate at which data can be transmitted through a standard 72-MHz-wide satellite-transponder channel.

The research revealed that the primary barriers to reducing the costs of high-rate modems lay in (1) expensive high-power amplifiers (HPAs) needed to support high rates and higher-order, more-bandwidth-efficient modulations; (2) expensive frequency converters that satisfy stringent phase-noise requirements; and (3) expensive high-resolution, high-rate analog-to-digital converters (ADCs). The research then focused on the development of modulation/demodulation and coding/decoding techniques to overcome each of these cost barriers.

One of the innovative features of the modem design is the use of pragmatic trellis coded modulation (PTCM) to reduce (1) the required power and other required performance parameters and thus (2) the cost of the power amplifier. The modem is capable of a fully rotationally invariant octonary-phase-shift-keying (8PSK) PTCM; this means that it is possible to flywheel through a cycle slip with no loss of data — a crucial benefit for Earth/satellite wireless data communications.

The design incorporates analog-matched-filtering and single-sample-per-baud concepts that, in combination, greatly reduce cost and complexity, relative to modems developed previously for the same purpose. The design supports low-complexity modulators by providing for square-root-Nyquist pulse shaping with programmable predistortion and programmable values of α. This programmability enables a communication-link designer to trade α and HPA backoff for a fixed baud rate to achieve the maximum possible data rate through a transponder channel.

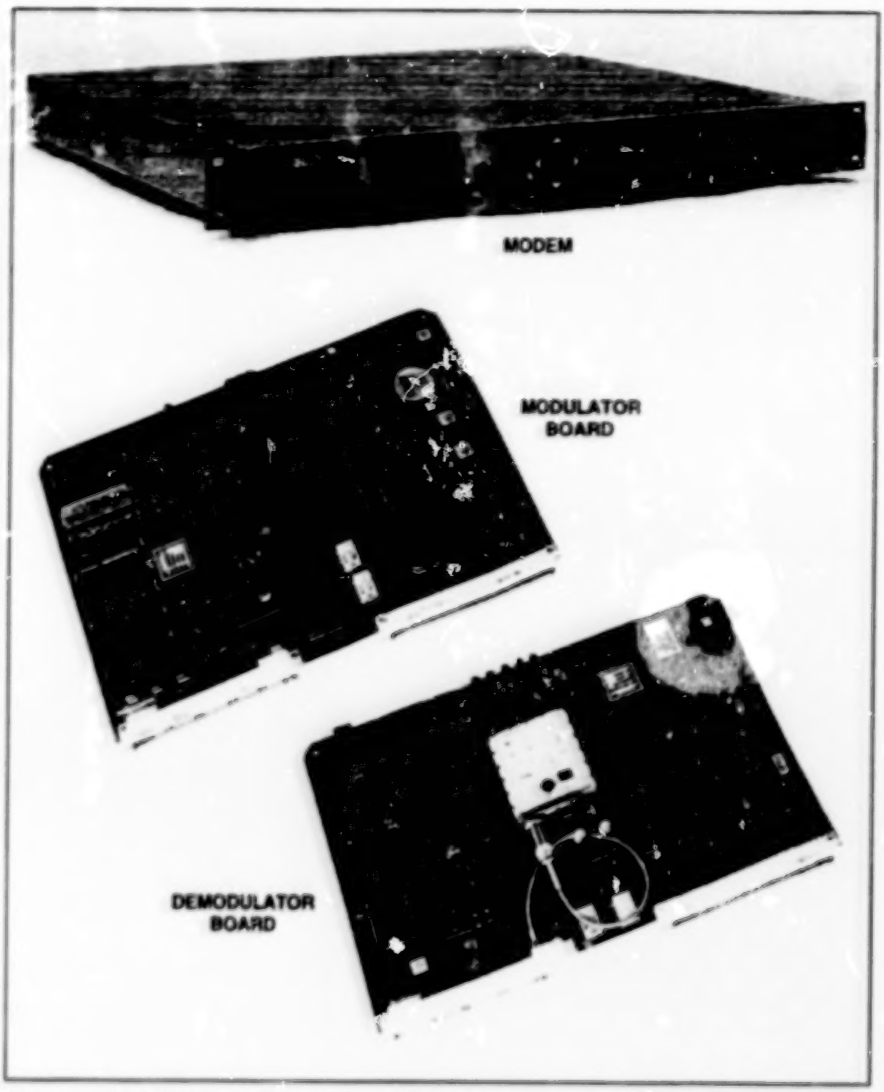

This **Low-Cost Modem** enables wireless digital communication at a rate up to 155.52 Mb/s. An even higher data rates can be achieved by operating multiple such modems in parallel.

Another innovative feature of this modem stands in contrast to the conventional means of converting a stream of 4 complex samples per baud into quadrature analog baseband waveforms. In the conventional approach, the streams are multiplexed and passed through a very fast digital-to-analog converter (DAC); not only is a fast DAC expensive, but the board and assembly costs are high because of the need to use emitter-coupled-logic components (latches, clock drivers, and so forth). In this modem, the conventional high-speed DAC is replaced with four baud-rate DACs, thereby effecting a significant reduction in cost. Moreover, unique data encoding and pulse shaping reduce (in comparison with that of a typical previously developed modulator) the maximum stop-band energy level by nearly 12 dB, further enhancing modulation quality.

In a comparative test against a state-of-the-art high-rate European modem, this modem demonstrated superior performance in the transfer of data through a satellite transponder, the ability to function properly with frequency translators that cost only 1/40 as much as do the frequency translators in the European modem, and an overall cost of one-fourth of that of the European modem. In other tests,

- Transfer of data at the design rate of 155.52 Mb/s was demonstrated in a

laboratory environment; and

- Transfer of data at a rate of 75 Mb/s was demonstrated through a 36-MHz-wide transponder channel, using a rate-5/6 PTCM and 8PSK.

The modem is also expected to support a 16-state quadrature amplitude modulation (16QAM), 155.52-Mb/s link, using a Reed-Solomon (187, 204) outer code and a rate-3/4 pragmatic trellis code. The link occupies a nominal frequency band 73.5 MHz wide, and it should be possible to accommodate the link in a standard 72-MHz-wide transponder channel; however, at the time of reporting the information for this article, a field test of the modem with such a link had not yet been performed.

This work was done by Ron McCallister, Bruce Cochran, and Jim Crawford of SICOM, Inc. for **Glenn Research Center.** *Further information is contained in a TSP [see page 1].*

Inquiries concerning rights for the commercial use of this invention should be addressed to NASA Glenn Research Center, Commercial Technology Office, Attn: Steve Fedor, Mail Stop 4–8, 21000 Brookpark Road, Cleveland, Ohio 44135. Refer to LEW-16668.

Improved HRTF-Based Pseudostereophony

Monaural signals are filtered digitally to obtain pseudostereophonic output signals.

Ames Research Center, Moffett Field, California

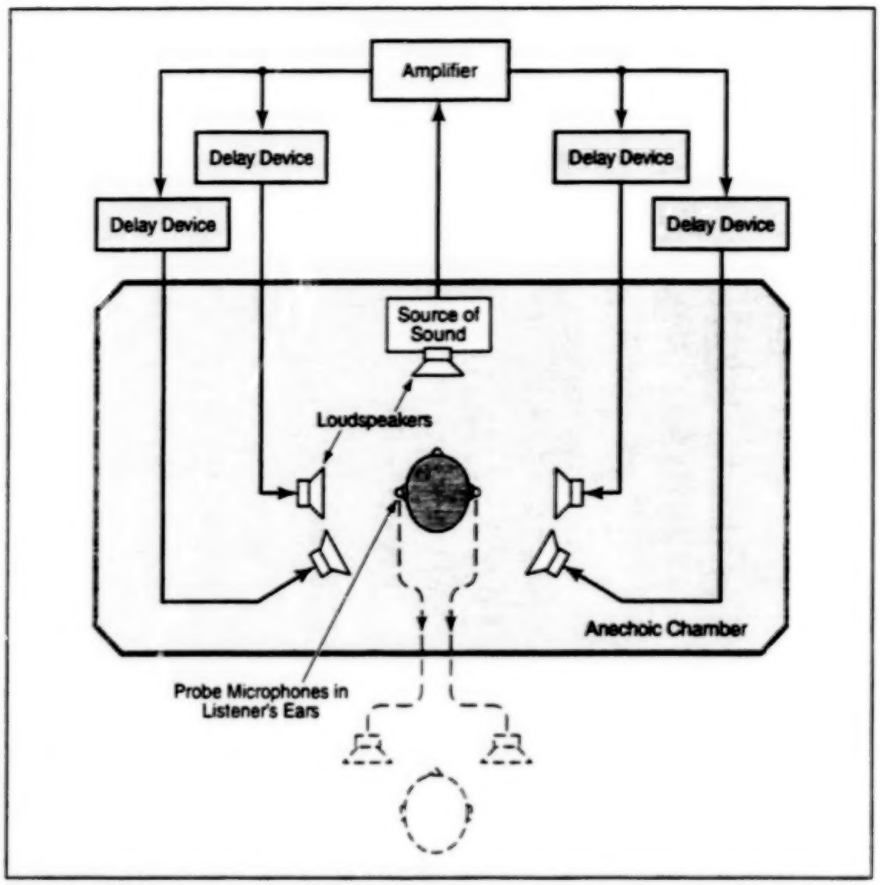

Figure 1. **Sounds Arriving in a Listener's Ears** from various directions are measured, then used to compute head-related transfer functions.

An improved pseudostereophonic system utilizes digital filtering and head-related transfer functions (HRTFs) to afford tailorability and sound quality not available from older pseudostereophonic systems. Although the term "pseudostereophony" may not be widely known, the underlying concept has been studied and applied for more than four decades. Pseudostereophony is a family of techniques for deriving right and left channels of sound from a single-channel (monaurally recorded) source to give the listener an impression of sound coming from more than one direction.

The pinnae of human ears affect entering sound in a way that varies with the direction of incidence and thus gives the brain cues to the location of the source. These cues are in addition to the directional cues provided by differences between the times of arrival of signals. The effects of the pinnae can be quantified by HRTFs. In the time domain, an HRTF is an impulse response, as a function of direction of incidence, that is convolved with the incident acoustic signal. In the frequency domain, the HRTF is a magnitude and phase response, as a function of frequency of sound and direction of incidence, that multiplies the frequency-domain complex-amplitude representation of the incident acoustic signal.

The present pseudostereophonic system utilizes HRTFs in the following way: First, the HRTFs of an average human listener are determined experimentally. Thereafter, the digital HRTFs are used, along with delays and optional filtering functions, to digitally synthesize right- and left-channel signals that make a listener perceive the sound as coming from multiple sources in different directions.

Figure 1 depicts an apparatus for measuring HRTFs for five directions of incidence. A human listener sits in an anechoic chamber, with a loudspeaker at ear height directly in front (azimuth 0°) and four other loudspeakers at ear height at azimuths of 90, 120, 240, and 270°. A source of sound is connected to the loudspeaker at 0° and is connected to the other loudspeakers through an amplifier and delay devices. Small probe microphones in the listener's ears measure the entering sound. In principle, as indicated by the dashed lines, the outputs of the right and left microphones could be simplistically fed to right and left loudspeakers, respectively, to generate sounds with perceived directional characteristics. However, instead, the sounds measured by the microphones are used to compute the HRTFs, which are then used

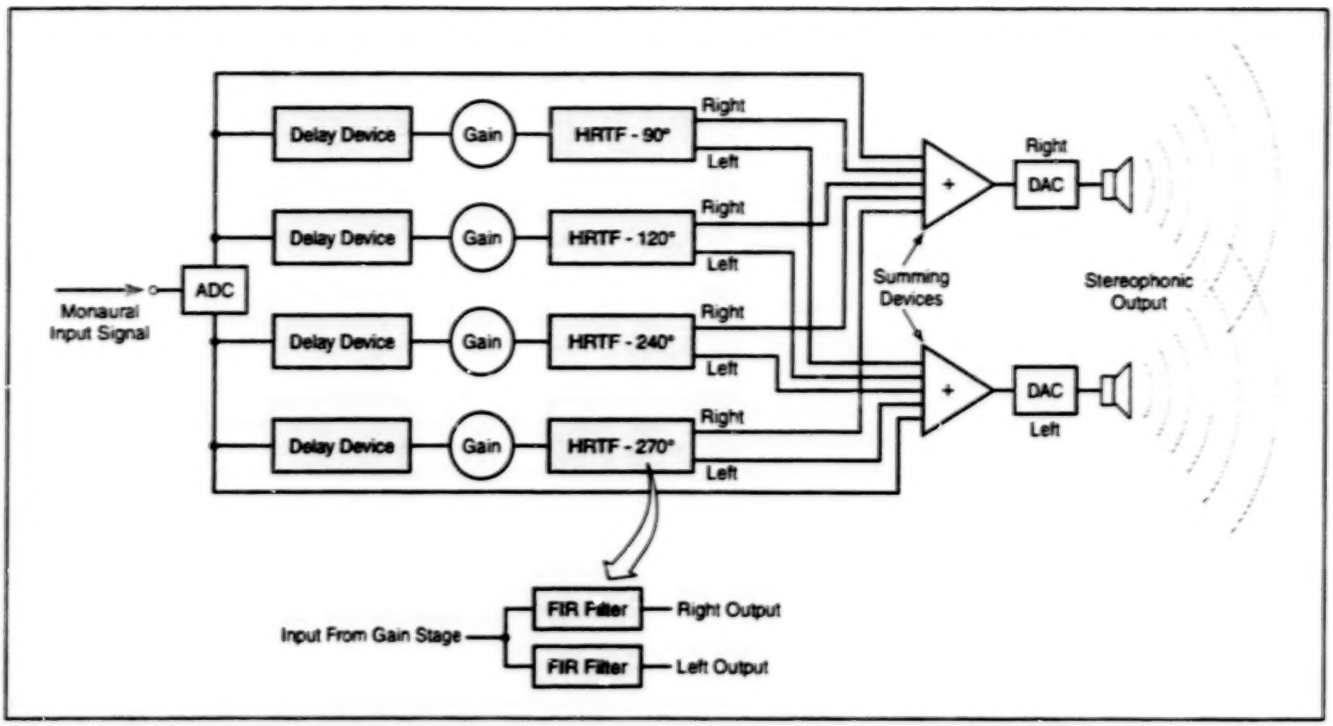

Figure 2. **A Monaural Signal Is Digitally Filtered** to synthesize right and left signals for a pseudostereophonic effect.

in the pseudostereophonic system depicted in Figure 2.

A monaural input signal is fed to an analog-to-digital converter (ADC). The digital signal is distributed on six lines. Lines 1 and 6 couple the signal directly to left and right digital summing devices, while each of lines 2 through 5 passes through an individual digital delay device that corresponds to one of the nonzero azimuth angles. The delays of these devices differ and are set as described below.

The outputs of all the delay devices are multiplied by a common gain factor that can be adjusted by the user. Next, each delayed and multiplied signal is processed by a right and a left finite-impulse-response (FIR) filter that approximates the right and left HRTF, respectively, for the azimuth angle. The resulting left and right HRTF outputs are summed in the left and right digital summing devices, respectively. The summed outputs for the left and right channels are then passed through separate digital-to-analog converters (DACs) to the left and right loudspeakers, respectively.

The delays, gains, and FIR-filter parameters can be chosen to obtain desired psychoacoustic effects. For example, the gain of the delayed signals on lines 2 through 5 can be set at 6 dB, in keeping with an empirical finding that this is the best gain for pseudostereophony with sounds of various types, including speech and music. Alternatively, the user can set the gain at zero for monaural listening, or can set the gain at >6 dB to obtain an exaggerated pseudostereophonic effect.

Criteria for setting delays are somewhat more complex. Parameters to be considered include (1) the interval between the undelayed sound and the first delay, (2) the intervals between succeeding delays, and (3) the time of the final delay, which depends on the previous delays. An important psychoacoustic consideration in choosing delays is that the signals remain below the level of echo disturbance; in this regard, the initial delay has been found to be the most important one. The intervals between successive delays should be within a range so that each delayed sound would not be heard as a separate sound. Typical acceptable values of initial delay are between 15 and 25 ms, and optimum intervals between successive delays are between 5 and 10 ms. In order for the use of HRTFs to yield a sensation of increased auditory spaciousness, the final delay should be at least 30 ms; this is consistent with findings from research into the effect of early reflections in concert halls.

Although the system as described thus far includes four delay and HRTF channels, it could also be constructed with more or fewer delay and HRTF channels. Other possible variations include the use of larger or smaller numbers of coefficients used to approximate the HRTFs in the FIR filters.

In comparison with older pseudostereophonic systems, this system generates sound that is less "colored"; that is, less altered in timbre. This system offers greater flexibility for synthesizing the sound at a wider range of listening positions. The two output channels of the present system can also be mixed to monaural output without disturbing coloration effects that result from phase cancellation. Moreover, the sound gives an increased impression of spaciousness because the two output signals are decorrelated. Yet another advantage is that multiple inputs with differential frequency responses can be distinguished from each other more easily in this system than in a monaural system.

This work was done by Durand R. Begault of **Ames Research Center**. *Further information is contained in a TSP [see page 1].*

This invention has been patented by NASA (U.S. Patent No. 5,173,944). Inquiries concerning nonexclusive or exclusive license for its commercial development should be addressed to the Patent Counsel, Ames Research Center [see page 1]. Refer to ARC-11919.

Microwave Battery Charger

Batteries would be kept charged without wire connections.

Goddard Space Flight Center, Greenbelt, Maryland

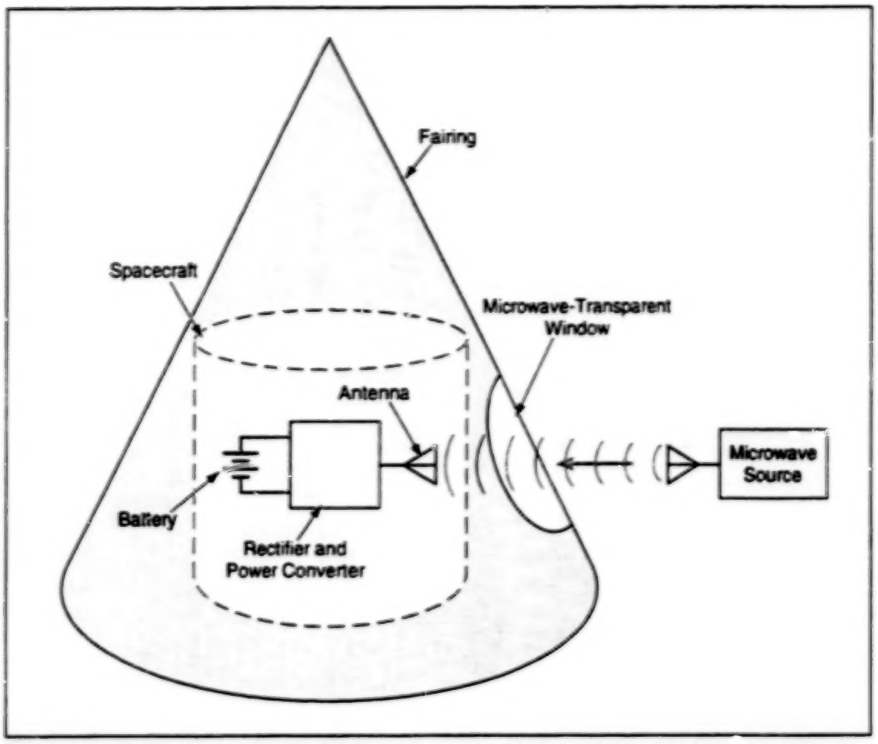

Microwave Power Would Be Rectified to dc power, which would be used to charge batteries.

A simple microwave power-transmission system has been proposed for maintaining the charge on spacecraft batteries immediately prior to launch. The basic concept of this system could also be applied to other systems (e.g., emergency equipment) that must be kept in a state of high readiness for rapid deployment, without need for cable connections that could impede or slow deployment.

The umbilical cable that supplies power to a spacecraft on a launch pad must be disconnected at some prescribed time before launch. Once the disconnection is made, the spacecraft operates on battery power. The spacecraft must be launched before the battery discharges so much that the spacecraft could not be relied upon to function correctly. The launch must be canceled if the delay exceeds the allowable discharge time.

The proposed system would make it unnecessary to cancel a launch on account of battery discharge. The system (see figure) would function as follows: Immediately before the disconnection of the umbilical cable, a microwave source would be turned on. The microwave beam from this source would be aimed at the spacecraft through a microwave-transparent window on the fairing of the launch rocket. An antenna on the spacecraft would intercept the microwave beam. A rectifier-and-power-converter circuit connected to the antenna would convert the received microwave power to dc power, which would be used to charge the spacecraft batteries.

This work was done by Richard Rolnicki of **Goddard Space Flight Center**. *No further documentation is available.*
GSC-13784

Imaging With a Focal-Plane Array of Ultrasonic Transducers

Phenomena that can be imaged include gas leaks, moving objects, and thermally induced air currents.

John F. Kennedy Space Center, Florida

A prototype system for acoustic imaging of gas leaks that emit ultrasound was developed at Kennedy Space Center. Potential government and commercial users concerned with leak imaging and safety expressed interest in this technology.

The prototype system includes an 8 × 8 array of air-coupled acoustic transducers with a peak-response frequency of 40 kHz. As indicated in the figure, the array is placed at the focal plane of a paraboloidal reflector (see figure) with a focal length of about 1 ft (30 cm). Thus, the array functions analogously to focal-plane arrays of photodetectors for imaging optical sources or focal-plane arrays of antenna elements for imaging radio sources, the unique feature of this array being that it provides a low-resolution image of acoustic sources in its field of "view."

The output signals from the transducers are buffered out serially through a 64-to-1 multiplexer, then sent to a microprocessor that includes an analog-to-digital converter. The microprocessor controls the operation of the multiplexer and sends the digitized, processed transducer outputs to a computer, which generates a real-time video display in which the intensities of the acoustic signals are represented by brightnesses in the cells (in effect, acoustic pixels) of a square 8 × 8 grid corresponding to the transducers. By use of a pixel-to-pixel-averaging algorithm, the pattern can be converted to one of 15 × 15 acoustic pixels with blocky appearance of the grid softened somewhat to give an appearance of finer resolution.

As described thus far, the system operates in a passive mode, in which it produces intensity images of leaks or other sources of high-pitch sound. However, the system also offers the more-powerful capability of operation in an active phase-imaging mode, in which the scene is "illuminated" by an ultrasonic signal of specified frequency and phase. Because the microprocessor has access to the phase as well as the magnitude or intensity information for each ultrasonic pixel, it is a relatively simple matter to process the transducer outputs to obtain an image in which the brightness of each ultrasonic pixel represents the difference between the phase of the "illuminating" signal and the signal returned to the corresponding transducer.

Phenomena that alter the speed of sound and thus the phase of the return signal can be imaged in this mode. Tests of the prototype system in the active phase-imaging showed it to be capable of imaging gas leaks, a cold airflow, and

moving objects. It should also be possible to image fires and temperature gradients in still or moving air.

Recent improvement included the following:

- Preventing the receiver from being overwhelmed by near-field reflections of the transmitted signal;
- Increasing the resolution by increasing the number of transducers, along with the size of the reflector and/or the frequency; and
- Designing alternative systems with wider fields of view.

This work was done by William D. Haskell, James P. Strobel, Robert C. Youngquist, John S. Moerk, and Robert B. Cox formerly of I-NET for **Kennedy Space Center**.

For further information, contact UE Systems, owner of the exclusive license:

UE Systems
14 Hayes Street
Elmsford, NY 10523-2536
Telephone No.: (914) 592-1220

KSC-11909

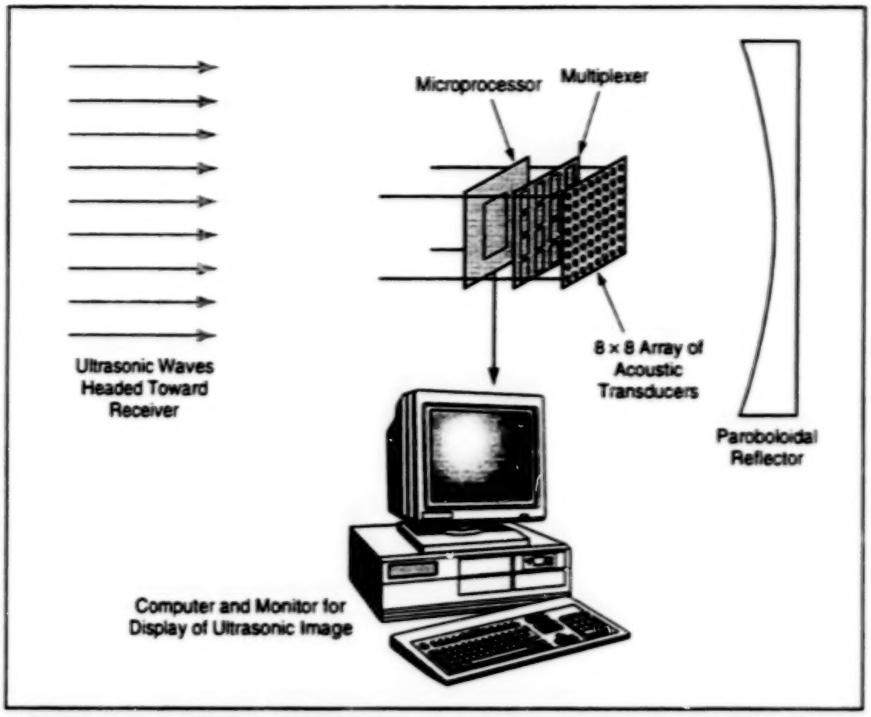
Microprocessor
Multiplexer
Ultrasonic Waves Headed Toward Receiver
8 × 8 Array of Acoustic Transducers
Paraboloidal Reflector
Computer and Monitor for Display of Ultrasonic Image

A Square Array of Acoustic Transducers at the focal plane of a paraboloidal reflector puts out signals that can be processed to form a crude image of a distant source of ultrasound.

BLANK PAGE

Physical Sciences

Hardware, Techniques, and Processes

21 Interferometric System Images Small Vibrating Structures
22 Exploiting Ion/Atom Cold Collisions in Atomic Clocks
23 Two-Photon Microscope Imaging Spectrometer

BLANK PAGE

Interferometric System Images Small Vibrating Structures

Stroboscopic interferograms depict surface profiles at selected phases of vibration.

NASA's Jet Propulsion Laboratory, Pasadena, California

A commercial scanning imaging white-light interferometer designed for measuring surface profiles of stationary objects has been modified into an interferometric instrument for imaging vibrating microelectromechanical structures. The modified instrument operates in a stroboscopic mode, generating a set of interferograms at a selected instant in the vibrational cycle. A number of sets of interferograms can be acquired at different instants of time corresponding to small increments of phase through the vibrational cycle so that the resulting collection of interferograms shows how the shape of the vibrating surface changes during the cycle; thus, the interferograms yield information on the shape and amplitude of the vibrational mode or modes.

The figure schematically illustrates the unmodified and modified versions of the instrument. The magnified image of the specimen is brought to focus in a charge-coupled-device (CCD) camera oriented along a main (vertical) optical axis. In the unmodified instrument, an incandescent lamp generates white light, which is reflected down along the main optical axis by a beam splitter. The microscope objective assembly contains another beam splitter, which divides the illumination into two beams: a reference beam sideways to the main optical axis and an object beam, which continues down along the main optical axis, through the objective lenses, and onto the specimen.

The reference beam is reflected from a flat mirror, then reflected from the beam splitter in the objective assembly back up the main optical axis toward the camera. The object beam is reflected from the specimen, passes up through the beam splitter and the lenses in the objective assembly, and into the camera. Interference between the object and reference beams forms the desired interference pattern on the focal plane of the camera.

The specimen is moved along the main optical axis, passing through the position of zero optical-path-length difference. CCD outputs representing interferograms are acquired and digitized at various increments of optical-path-length difference. Then by use of special-purpose software, the digital interferograms are used to compute the surface profile of the specimen. The unmodified instrument cannot be used to obtain the surface profile of a vibrating specimen because the vibration blurs the interference patterns.

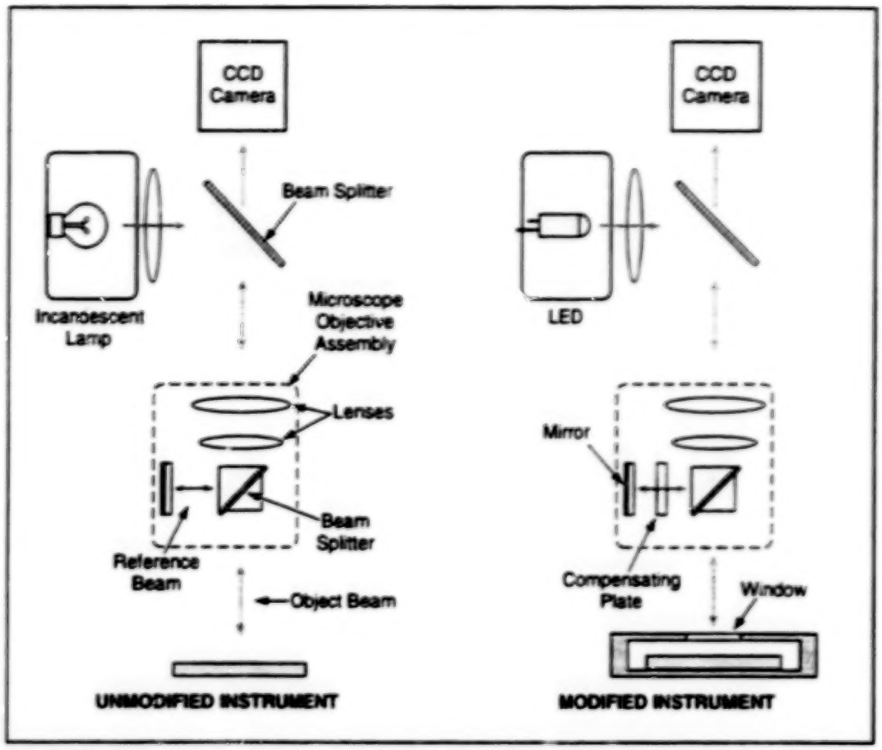

The Basic Optical Instrument — in both the unmodified and modified versions — is a low-magnification microscope combined with a Michelson interferometer.

In the modified instrument, the incandescent lamp is replaced by an ultrabright light-emitting diode (LED), which can be driven by pulses at a repetition rate up to 2 MHz. The pulse generator that drives the LED is synchronized to the function generator that drives the vibrations of the specimen. The phase-offset capability of the function generator is used to select the increments of phase for acquiring sets of interferograms.

Because of the viscous drag, many microelectromechanical structures do not vibrate in air at atmospheric pressure. Therefore, in the modified instrument, the specimen is mounted in a small vacuum chamber and observed through a window. To compensate for the optical path length through the window, the modified instrument includes a plate of the same optical thickness as that of the window inserted in path of the reference beam.

With the modified instrument, vibrational displacements along the main optical axis can be measured with resolutions of the order of nanometers. The only fundamental limitation of the modified instrument lies in the competing requirements for stroboscopic illumination: One must generate enough luminous energy during each pulse to obtain an image, while keeping the pulse short enough, to prevent motion blur of the image. "Short enough" as used here is defined with respect to the amplitude and frequency of the vibration and means, specifically, that the displacement during the pulse must be no more than about 1/20 of the wavelength of the light from the LED.

This work was done by Roman Gutierrez, Kirill Shcheglov, and Tony K. Tang of Caltech for **NASA's Jet Propulsion Laboratory**. *Further information is contained in a TSP [see page 1].*

NPO-20177

Exploiting Ion/Atom Cold Collisions in Atomic Clocks

Laser-cooled neutral atoms would be used to cool ions and perform other functions.

NASA's Jet Propulsion Laboratory, Pasadena, California

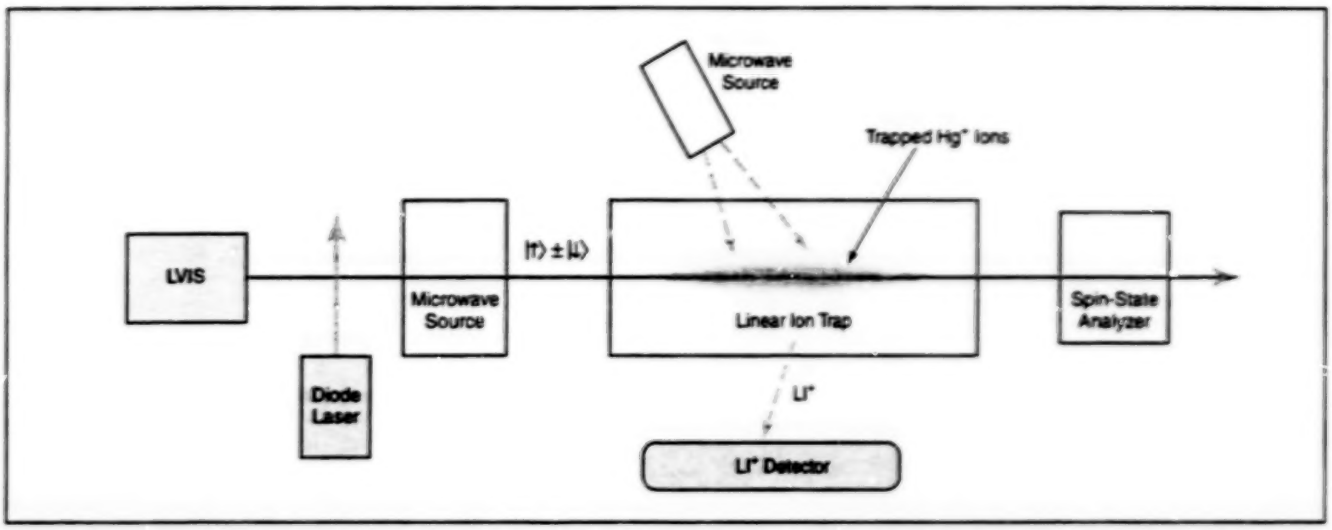

Lithium Atoms Would Be Cooled by laser beams in the LVIS. The resulting beam of lithium atoms would be spin-polarized by optical pumping on its way to the linear ion trap, where it would cool and spin-polarize the $^{199}Hg^+$ ions. Li^+ ions generated as a byproduct of the microwave-induced transition in the $^{199}Hg^+$ ions would be ejected and detected. Depolarization of the beam of lithium atoms could be detected in a spin-state analyzer by optical fluorescence following excitation by a diode laser.

Recent advances in laser cooling and trapping of neutral atoms in magneto-optic traps (MOTs) would be exploited in ion-trap-based atomic clocks, according to a proposal. Beams of laser-cooled neutral atoms would be used to: (1) put the ions in the required quantum states (e.g., spin-polarize the ions) in preparation for quantum state transitions that define the clock frequencies, (2) cool the trapped ions to reduce clock instabilities from second-order Doppler shifts of clock frequencies, and (3) monitor the clock quantum state transitions. The cooling, state preparation, and monitoring would occur via ion/atom collisions.

The proposal is based on a complex of interdependent physical phenomena that include elastic and inelastic collisions among ions and neutral atoms, electric polarization of neutral atoms by nearby ions, spin-exchange and charge-exchange reactions among neutral atoms and ions, and radiative state transitions. For the sake of brevity, the proposal is described below by way of an example; how it would be applied to an atomic clock based on $^{199}Hg^+$ ions in a linear ion trap.

Atomic clocks of this type were described in several previous articles in *NASA Tech Briefs*. To recapitulate; a clock of this type includes a microwave local oscillator, the frequency of which is stabilized by comparison with the frequency (about 40.5 GHz) of a ground-state hyperfine transition of $^{199}Hg^+$ ions. The ions are held in a linear ion trap to obtain a long interrogation time and thus a high resonance quality factor. Heretofore, the cooling of ions and the comparison of frequencies has involved a combination of ultraviolet (wavelength = 194 nm) and microwave excitation and interrogation of the ions. The generation of the excitatory ultraviolet light is difficult and expensive because one must use multiple visible lasers that generate watts of power, together with delicate frequency-doubling crystals.

The proposal would eliminate the need for the ultraviolet light. The proposal is based partly on the observation that it would be easier and less expensive to use small diode lasers to generate visible light and use this light to cool neutral Li atoms in an MOT. The light from the laser diodes would be carried by optical fibers and split into three intersecting, retroreflected, circularly polarized beams that would effect the cooling in the MOT; this would all be accomplished by use of off-the-shelf components.

The figure schematically depicts an apparatus that would be used to test the proposal. The MOT would be the heart of a low-velocity intense source (LVIS) of a cold beam of neutral Li atoms. The beam would be directed into the linear ion trap of an atomic clock. In the trap, the $^{199}Hg^+$ ions would be cooled and state-prepared via collisions with the neutral Li atoms. Li^+ ions would be generated as byproducts of a spin-dependent charge-transfer interaction that would occur as a result of the microwave-induced clock transition in the $^{199}Hg^+$ ions. In the radio-frequency electric field that traps the $^{199}Hg^+$ ions, the motion of the Li^+ ions would be so great that the Li^+ ions would be immediately ejected from the trap. The ejected Li^+ ions could thus be used to indicate the clock transition; for this purpose, the ejected Li^+ ions could be detected by channeltron electron multipliers surrounding the trap. Assuming detection of all ejected Li^+ ions, the short-term clock stability has been estimated to be $\approx 10^{-14}\tau^{-1/2}$, where τ is the averaging time in seconds.

This work was done by John Prestage of Caltech for **NASA's Jet Propulsion Laboratory**. *Further information is contained in a TSP [see page 1].*

NPO-20365

Two-Photon Microscope Imaging Spectrometer

Overlapping spectra from fluorescent-dye probes could be separated.

NASA's Jet Propulsion Laboratory, Pasadena, California

A two-photon microscope imaging spectrometer has been proposed for use in scanning confocal two-photon microscopy. The proposed instrument would solve a spectrum-overlap that sometimes arises, as explained below.

Scanning confocal two-photon microscopy is a variant of fluorescence microscopy, in which fluorescent dyes are used as probes for selective monitoring of biological compounds and cells. In scanning two-photon confocal microscopy, a specimen is raster-scanned by a laser beam that is focused into the specimen through the objective lens of a microscope. Fluorescent light excited by two-photon absorption is collected by a photodetector. Light is collected from each pixel, then the output of the photodetector is digitized and stored. This process is repeated for all the pixels in the raster scan, thereby building up a digitized image that represents an "optical section" that is, in effect, a fluorescence cross section in the focal plane. Further repetition of the process on a succession of closely spaced focal planes yields three-dimensional image data.

If multiple dyes with overlapping fluorescence spectra are used, then one is faced with the problem of how to separate the individual fluorescence images, each of which reveals a different aspect of the structure and function of the specimen. The problem could be solved by processing image data acquired by the proposed two-photon microscope imaging spectrometer. The fluorescence-image data generated by this instrument would be resolved not only spatially but also spectrally; that is, a spectrum would be acquired for each pixel. If the spectrum of each pixel were a sum of overlapping, known fluorescence spectra, then by use of previously developed spectral-data-processing techniques, the intensity of each fluorescence spectrum (and thus the abundance of the corresponding dye in the pixel) could be computed.

In one version of the proposed instrument, a tunable filter (e.g., a liquid-crystal tunable filter) would be placed in front of the photodetector and would be tuned across the wavelength range of interest to acquire a spectrum for each pixel. One potential disadvantage of this version is that the spectrum-acquisition time could be long enough that one or more fluorescent dye(s) in the specimen could become photobleached during the concomitant long exposure to the laser beam used to excite the fluorescence. A second major problem is that the data acquisition time is too long for many biological problems.

A second version of the instrument would operate with a shorter exposure time per pixel, and thus less photobleaching. In this version, the fluorescent light from each pixel would be focused onto the entrance slit of a spectrometer. Inside the spectrometer, the light would be dispersed by wavelength along a linear array of photodetectors. To obtain sufficient sensitivity to acquire the spectrum for each pixel in a sufficiently short time, the array of photodetectors would likely have to consist of multiple photomultiplier tubes, a multielement photomultiplier tube, or an intensified charge-coupled-device (CCD) array.

This work was done by Gregory Bearman, Scott Fraser, and Rusty Landsford of Caltech for **NASA's Jet Propulsion Laboratory**. *Further information is contained in a TSP [see page 1].*

In accordance with Public Law 96-517, the contractor has elected to retain title to this invention. Inquiries concerning rights for its commercial use should be addressed to

Technology Reporting Office
JPL
Mail Stop 122-116
4800 Oak Grove Drive
Pasadena, CA 91109
(818) 354-2240

Refer to NPO-20533, volume and number of this NASA Tech Briefs *issue, and the page number.*

BLANK PAGE

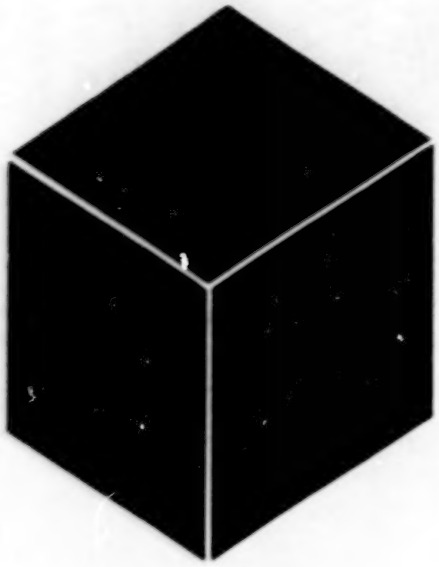

Materials

Hardware, Techniques, and Processes

27 Susceptor-Coating Materials for Growth of 4H-SiC
27 Priming Ceramic Materials for Better Waterproofing
28 Improved Fabrication of $YBa_2Cu_3O_{7-x}$ Superconductors

Books and Reports

28 Reaction-Forming Method for Joining SiC-Based Parts

BLANK PAGE

Susceptor-Coating Materials for Growth of 4H-SiC

Better coatings are needed to obtain precise C/Si concentrations and minimize contamination.

John H. Glenn Research Center, Cleveland, Ohio

Several materials have shown promise for coating graphite susceptors used in epitaxial growth of 4H-SiC. The development of appropriate susceptor-coating materials is an essential part of continuing efforts to produce high-quality, thick, undoped and lightly doped epilayers of 4H-SiC for use as semiconductors in future electronic devices that will operate at power levels and temperatures beyond the limits of Si- and GaAs-based devices.

SiC grows in many different crystalline structures called "polytypes." 4H-SiC is one of these polytypes and is the preferred one for electronic devices because in comparison with other SiC polytypes, its charge-carrier mobility is greater and the anisotropy of its mobility is smaller. Epitaxial films of SiC are made by chemical vapor deposition (CVD) from carbon- and silicon-containing gas mixtures onto radio-heated susceptors. Heretofore, the most common susceptor materials have been graphite and SiC-coated graphite.

The input flows of Si- and C-containing gases into an SiC CVD chamber are well controlled by use of mass-flow controllers, but this does not always suffice to achieve the needed precise control of the proportion of C to Si. Both bare graphite and SiC-coated graphite susceptors are vulnerable to etching at the growth temperature (typically >1,350 °C) in the presence of H_2, which is one of the gases in a typical CVD gas mixture. Depending on the susceptor material and the particular CVD process, such etching releases uncontrolled amounts of C and/or Si into the CVD gas mixture, thereby giving rise to undesired changes in the structure, density of defects, and doping of the epilayer. Etching of a graphite susceptor can also release B, Al, and other impurities that can become incorporated into the epilayer as undesired dopants. Moreover, a bare graphite susceptor is porous and can trap a desired dopant during a CVD run, then release the dopant during a subsequent CVD run, in which the dopant could be undesired.

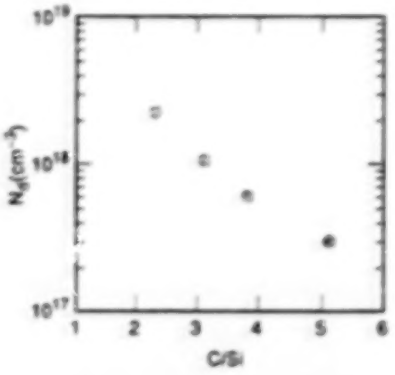

A 4H-SiC Epilayer was grown by CVD, using a carbon-based coating on a graphite susceptor. An 11.5-μm thick epilayer showed a smooth surface morphology, and n-type doping control via site competition epitaxy was demonstrated as shown.

Thus, a graphite-susceptor-coating material that is much less vulnerable to etching is needed for growing high-quality 4H-SiC. A suitable material must have a coefficient of thermal expansion close to that of the underlying graphite, must adhere to the graphite without flaking or chipping off during CVD, must be sufficiently thermally conductive to transfer heat from the susceptor to the growing epilayer, must be amenable to deposition in a layer thin enough not to obstruct coupling of radio-frequency energy to the susceptor, should have low porosity to prevent trapping of impurities, and should be as chemically inert as possible in the presence of hot H_2.

Four materials that satisfy these criteria to various degrees were selected as candidates for experimental evaluation. One of these materials was SiC, which as reported above, was already known to be vulnerable to etching. The other materials were carbon-based coatings, denoted as C1, C2, and C3. The C1 coating was used to establish an epitaxial-growth baseline for comparisons. The films grown with SiC-coated graphite susceptors were of poor quality in comparison with those grown on the C1-coated susceptors, and the SiC-coated susceptors were severely degraded, leading to the conclusion that SiC should be excluded from further consideration. On the other hand, the SiC films produced with the C2- and C3-coated susceptors were of high quality, and the doping control was demonstrated (see figure). The C2-coated susceptors exhibited no obvious degradation and appeared to have operational lifetimes longer than those of the baseline C1-coated susceptors. The C3-coated susceptors exhibited some chipping. These results suggest that these carbon-based coatings could be suitable for epitaxial growth of high-quality 4H-SiC.

This work was done by Barbara Landini of Advanced Technology Materials, Inc., for **Glenn Research Center**. *No further documentation is available.*

Inquiries concerning rights for the commercial use of this invention should be addressed to NASA Glenn Research Center, Commercial Technology Office, Attn: Steve Fedor, Mail Stop 4–8, 21000 Brookpark Road, Cleveland, Ohio 44135. Refer to LEW-16699.

Priming Ceramic Materials for Better Waterproofing

Precoating with silica facilitates the application of a waterproofing final coat.

Ames Research Center, Moffett Field, California

An improved process for waterproofing ceramic materials — especially lightweight ceramic insulation materials in both rigid (tile) and flexible (blanket) form — has been invented. In this process, traditional waterproofing agents are used, but before the waterproofing agents are applied, the ceramic substrates are first coated with thin layers of silica, as explained below.

As used here, "waterproofing" of ceramics means rendering them water-repellent, not making them impervious. In situations in which ceramics are exposed to water, the need for waterproofing arises as follows: These materials are very porous (void volumes exceed 90 percent in some cases). They are also hygroscopic — typically capable of absorbing three to five times their own weight of water. Water can thus add undesirably to the weight of these materials. These materials can also be damaged by explosive vaporization of trapped water during rapid heating, and by the anomalous expansion and contraction

of trapped water during freezing and thawing. Thus, what is needed is a means to reduce the intrusion of water to minimize these deleterious effects.

The traditional waterproofing agents preferred for this purpose are silanes, substituted silanes, silazanes, and mixtures of these. These agents can be applied easily to silica ceramics, but cannot be applied easily to other (e.g., alumina) ceramics. The present invention is based on the discovery that even a difficult-to-coat ceramic can easily be coated with a traditional silicon-containing waterproofing agent, provided that it is first coated with a thin layer of silica. "Coated" as used here does not mean covered on the exterior macroscopic surface; it means covered on all microscopic exterior and interior pore surfaces and interstices.

The silica coating is formed by first coating with a silica precursor and converting the precursor to silica either *in situ* during the coating process or subsequently by oxidative pyrolysis. Some of the traditional waterproofing agents mentioned above are also useful as silica precursors; other silica precursors include silicones and siloxanes. A silica precursor can be applied to a ceramic substrate by any of a number of techniques; for example, solution coating, vapor deposition, low-pressure chemical deposition, immersion, or injection. The silica coating is typically thin enough (thickness of the order of 1 μm or less) to be flexible, so that it can be used on either a rigid or a flexible ceramic substrate without risk of cracking and consequent exposure of the ceramic to moisture.

In an experiment to demonstrate the invention, a piece of ceramic insulation containing alumina batting was coated by contact with methyltrimethoxysilane vapor (the silica precursor), then further coated with dimethylethoxysilane waterproofing agent. The piece was then heated in air at 1,000 °C for two hours, destroying the waterproofing and pyrolyzing the silica precursor to silica. The waterproofing agent was then reapplied. The waterproofed piece was found to absorb less than 5 percent of its weight in water — an acceptably small amount of water in the application for which this particular piece of insulation was designed.

This work was done by Domenick A. Cagliostro and Ming-ta S. Hsu of **Ames Research Center**. *Further information is contained in a TSP [see page 1].*

This invention has been patented by NASA (U.S. Patent No. 5,814,397). Inquiries concerning nonexclusive or exclusive license for its commercial development should be addressed to the Patent Counsel, Ames Research Center [see page 1]. Refer to ARC-14029.

Improved Fabrication of $YBa_2Cu_3O_{7-x}$ Superconductors

These superconductors are made from pressed powders of Y_2O_3, CuO, and $Ba(NO_3)_2$.

Marshall Space Flight Center, Alabama

An improved method of manufacturing high-temperature superconductors of general composition $YBa_2Cu_3O_{7-x}$ and various grain structures has been devised. This method involves mixing, pressing, and heating of Y_2O_3, CuO, and $Ba(NO_3)_2$ powders. This method is easier than an older method that involved mixing and sintering of Y_2O_3, CuO, and $BaCO_3$ powders followed by repeated grinding and sintering, followed by pressing to final size and shape.

In the present method, the first step is to mix commercial grade powders of Y_2O_3, CuO, and $Ba(NO_3)_2$ by percent by weight of the final mixture. Optionally, the powder mixture can be doped with a small proportion of silver (such doping results in, among other things, a higher-density final product). The powder mixture is placed in a die and pressed at either room temperature or an elevated temperature. Pressing densifies the powder mixture and forms a piece of approximately final size and shape.

Both cold and hot pressing yield similar results, though hot pressing is ordinarily preferable because it results in a piece that is denser and less delicate and thus easier to handle. The denser hot pressed samples also maintain closer to the final desired shape. In the case of hot pressing, care must be taken not to exceed the peritectic-transformation temperature-and-pressure range of the powders because, if such a transformation occurs, then the powders react prematurely with each other and/or react with the die.

The pressed piece is taken from the die and placed on a substrate of densified aluminum oxide or other suitable material in a furnace. The temperature-vs.-time schedule of the furnace can be altered to obtain desired results. The best results occur when the temperature of the pressed piece is heated slowly to 550 °C and held there for one hour before raising the temperature slowly to 650 °C. Thereafter, to obtain the desired grain structure and quality, the pressed piece can be treated by almost any temperature-vs.-time profile or post-sintering procedure (for example, annealing in oxygen) cited in any of the numerous patents and research papers that address the manufacture of $YBa_2Cu_3O_{7-x}$ high-temperature superconductors.

A piece of bulk superconductor made according to this method can be used as is, provided that it has the desired final size and shape. Alternatively, it can be processed further; for example, it could be ground into a $YBa_2Cu_3O_{7-x}$ that could be further pressed and sintered to final size and shape.

This work was done by Glen A. Robertson of **Marshall Space Flight Center**.

This invention is owned by NASA, and a patent application has been filed. For further information, contact Sammy Nabors at (256) 544-5226 or sammy.nabors@msfc.nasa.gov. Refer to MFS-31284.

Books and Reports

Reaction-Forming Method for Joining SiC-Based Parts

Two reports present additional details about the method described in "Reaction-Forming Method for Joining SiC-Based Ceramic Parts" (LEW-16661), *NASA Tech Briefs*, Vol. 23, No. 3 (March 1999), page 50. To recapitulate: A carbonaceous mixture (typically a paste) is applied to a joint between parts. The parts are clamped together and heated to a temperature of 115±5 °C for 10 to 20 minutes; this action partly cures the mixture, gluing the parts together with just enough strength that one need not clamp the parts during subsequent processing. Silicon or a silicon alloy in tape, paste, or slurry form is applied to the joint region. The parts are heated to a temperature between 1,250 and 1,425 °C for 5 to 10 minutes, causing the silicon or

silicon alloy to melt, infiltrate the joint, and react with carbon. The finished joint, which is typically as strong as the parent material, contains silicon carbide with silicon and other phases. The amounts of the phases can be adjusted, by choice of the compositions of the reactants, to obtain joints with tailorable microstructures and thus tailorable thermomechanical properties.

This work was done by Mrityunjay Singh of NYMA, Inc., for **Glenn Research Center**. *To obtain copies of the reports, "A New Approach to Joining of Silicon Carbide-Based Materials for High Temperature Applications" and "Affordable, Robust Ceramic Joining Technology (ARCJoinT),"* *see TSP's [page 1].*

Inquiries concerning rights for the commercial use of this invention should be addressed to NASA Glenn Research Center, Commercial Technology Office, Attn: Steve Fedor, Mail Stop 4–8, 21000 Brookpark Road, Cleveland, Ohio 44135. Refer to LEW-16827.

BLANK PAGE

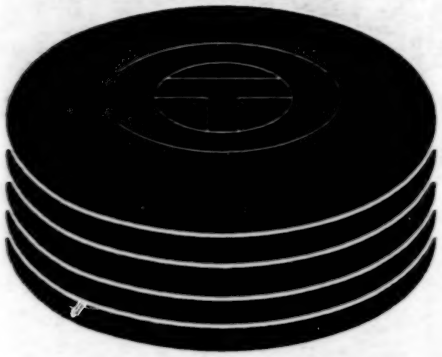

Computer Programs

Electronic Systems

33 Program for Analysis of Spacecraft Telecommunication Systems

Mathematics and Information Sciences

33 Software for Spacecraft/Ground Communication via the Internet

BLANK PAGE

Electronic Systems

Program for Analysis of Spacecraft Telecommunication Systems

A computer program facilitates the analysis and design of a radio-communication system for transmitting data from an orbiting spacecraft to ground stations. Input data provided by the user include primarily (1) parameters of the spacecraft orbit (including parameters that specify its position and orientation with respect to a coordinate system that translates with, but does not rotate with, the Earth); (2) either a specification of the gain pattern or else parameters needed to calculate the gain pattern of the antenna aboard the spacecraft; (3) type of spacecraft antenna aiming (nadir-pointed or articulated); (4) locations of the ground stations; (5) downlink bit rates and frequencies; (6) spacecraft instrument data rates; and (7) the angle (relative to the horizon) below which the line of sight from the spacecraft to each ground station is deemed to be blocked. The program calculates the spacecraft trajectory, the times when the spacecraft is visible from each ground station, the times (as functions of visibility and the antenna gain pattern) when radio communication is possible, the number of bits that a ground station can receive from the spacecraft during a given orbit, and the spacecraft data-storage capacity needed to hold data that are generated between communication intervals.

This work was done by Anil Kantak and Faiza Lansing of Caltech for **NASA's Jet Propulsion Laboratory**. *Further information is contained in a TSP [see page 1].*

This software is available for commercial licensing. Please contact Don Hart of the California Institute of Technology at (818) 393-3425. Refer to NPO-20672.

Mathematics and Information Sciences

Software for Spacecraft/Ground Communication via the Internet

The Space Communications Protocol Standards (SCPS) specify a developmental system of international protocols for data communications between spacecraft and points on Earth. SCPS protocols are intended to make a spacecraft appear, to a terrestrial computer user, as just another node on the Internet. The protocols are implemented to be as interoperable as possible to other systems. The SCPS file protocols are based partly on the Internet File Transfer Protocol (FTP), but include additional features necessary for smooth communication over channels that include interruptible Earth/spacecraft links; unlike the Internet FTP, the SCPS protocols provide for restart of interrupted file transfers and provide record read/update services. The SCPS protocols include (1) a file-handling protocol based on the Internet FTP, with modifications to optimize performance for typical spacecraft data streams; (2) an underlying retransmission protocol based on the Internet Transmission Control Protocol (TCP), with modifications to ensure reliability in the face of interruptions; (3) a data-protection protocol derived from a number of security protocols; and (4) a scalable networking protocol for routing of messages, based on the Internet Protocol (IP), with modifications to support space routing and increase communication efficiency.

This program was written by Eric Travis, Robert Durst, Patrick Feighery, and Mary Jo Zukoski of Mitre Corp. and by Steven Sides of SAIC for **NASA's Jet Propulsion Laboratory**. *Further information is contained in a TSP [see page 1].*

This software is available for commercial licensing. Please contact Don Hart of the California Institute of Technology at (818) 393-3425. Refer to NPO-20282.

34

BLANK PAGE

Mechanics

Hardware, Techniques, and Processes

37 Control Methodology To Alter Automobile Rollover Tendencies
37 Failure-Resistant Multiline Tethers
38 Program for Computing Dynamics of Multiple Bodies
39 Program Simulates Flights of Advanced Aerospace Vehicles

Books and Reports

39 Spacecraft Solar-Wind Trim Panels for Pointing

BLANK PAGE

Control Methodology To Alter Automobile Rollover Tendencies

Dynamics would be altered to effect safer distribution of loads to wheels.

NASA's Jet Propulsion Laboratory, Pasadena, California

A methodology of active control has been developed in an effort to alter (preferably to reduce) the tendency of a four-wheel land vehicle to roll over during tight turns and similar maneuvers. At the time of reporting the information for this article, hardware and software to implement the methodology were undergoing development and testing for incorporation into a variable-dynamics testbed vehicle (VDTV) — an experimental automobile that will be capable of exhibiting a broad range of dynamic characteristics for research on crash avoidance and driving-related human factors.

The VDTV will have four-wheel steering, front and rear active antiroll-bar systems, four adjustable dampers, and other active control devices that will be controlled by a computer running algorithms based on mathematical models of the dynamics of the vehicle. These devices will be used to alter several rollover-related characteristics of the dynamics of the vehicle, including notably its understeer coefficient, front/rear load-transfer distribution in lateral maneuvers that involve high accelerations, and the frequency and damping coefficient of the vehicle roll mode. Load-transfer distributions are particularly significant because to prevent rollover, one must ensure that the load on any tire never approaches zero during a severe maneuver.

A study has been performed to investigate how changes in the algorithms that control the active devices could effect significant changes in these characteristics. In particular, the study focused on how (1) an increase in the stiffness of the front antiroll bar, in conjunction with an increase in the front damper rate and with out-of-phase rear steering, could increase resistance to rollover in high-acceleration lateral maneuvers without changing the vehicle understeer coefficient (see figure); and (2) conversely, an increase in the stiffness of the rear antiroll bar, in conjunction with decrease in the rear damper rate and with in-phase rear steering, could decrease resistance to rollover. The results of the study indicate that the design of the VDTV provides for the right combination of active devices that will make the VDTV an effective testbed for research on rollover-related human factors.

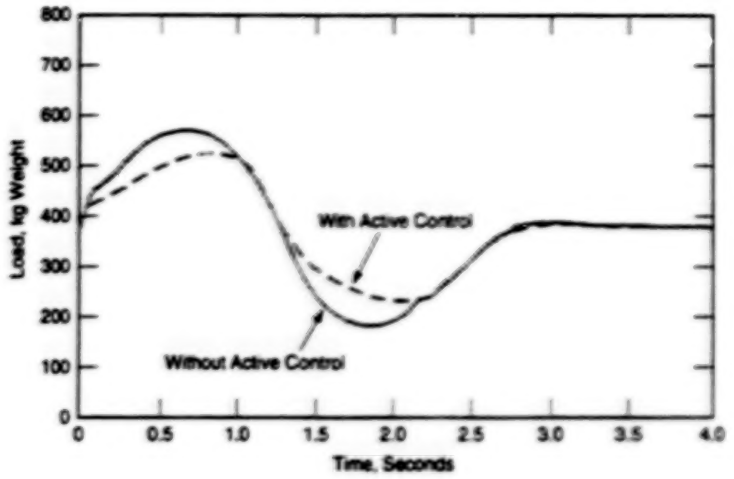

The Load on the Left Rear Tire of the VDTV was simulated by computer for a two-lane-change maneuver. By use of active control to increase the stiffness of the front antiroll bar, the minimum load at an extreme point of the maneuver was increased, thereby increasing the margin against rollover.

This work was done by Allan Y. Lee of Caltech for **NASA's Jet Propulsion Laboratory**. *Further information is contained in a TSP [see page 1].*

NPO-20545

Failure-Resistant Multiline Tethers

Secondary lines take up the slack when primary lines are severed.

Marshall Space Flight Center, Alabama

Hoytethers™ are failure-resistant multiline tethers named after their inventor, Robert Hoyt. They were originally intended for use in outer space to provide reliable tethering of satellites in the presence of orbital-debris and micrometeorite impacts that can sever single-line tethers. Hoytethers™ may also be adaptable to terrestrial use as tensile structural members in situations in which high reliability is required, such as climbing ropes, suspension bridges, and towering cables.

The basic failure-resistant multiline tether structure (see figure) is an open net comprising primary and secondary lines that, together, provide redundant linkage. Each primary line runs the full length of the tether and is anchored at both ends on a ring or bar that enforces the circumferential spacing (for a tubular tether) or lateral spacing (for a tape tether). The primary lines are connected diagonally at regular spatial periods by the secondary lines, which are attached firmly by braiding, twisting, clamps or other knotless interconnection methods, so as not to slip.

The secondary lines remain slack as long as the tether is undamaged. When a primary line is severed, the secondary lines assume the tensile load and redistribute the load in such a way that the effects of damage are localized to the vicinity of the cut. Although the secondary lines are diagonal, they lie nearly parallel to the primary lines. Therefore, the structure necks down only slightly when secondary lines take up the load from a damaged primary line and, as a consequence, the structure remains an open net, even in the vicinity of a cut. Thus, a small flying object that could sever a single line in the tether is still unlikely to cause total failure of the tether, even if it strikes in the vicinity of a previous cut.

Numerical simulations and experiments have confirmed the expectation of the inherent ability of these tethers to redistribute loads around severed primary lines and to maintain spacing between primary lines without need for rigid braces. The simulations and experiments have shown that these multiline tethers can withstand multi-

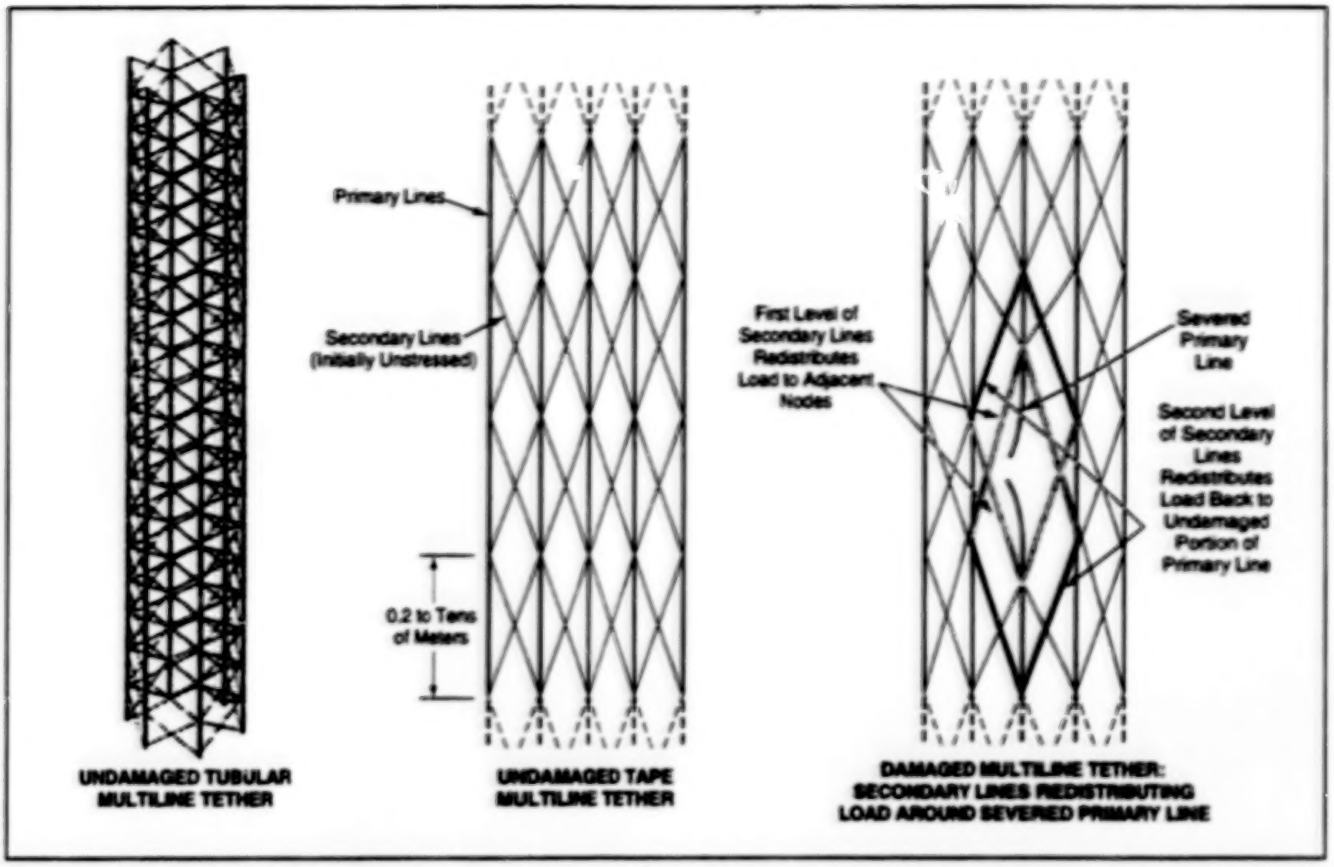
Primary Lines
Secondary Lines (Initially Unstressed)
0.2 to Tens of Meters
First Level of Secondary Lines Redistributes Load to Adjacent Nodes
Severed Primary Line
Second Level of Secondary Lines Redistributes Load Back to Undamaged Portion of Primary Line
UNDAMAGED TUBULAR MULTILINE TETHER
UNDAMAGED TAPE MULTILINE TETHER
DAMAGED MULTILINE TETHER: SECONDARY LINES REDISTRIBUTING LOAD AROUND SEVERED PRIMARY LINE

Secondary Lines Redistribute the Load around a cut in a primary line. The angles of the secondary lines are exaggerated in these views for the sake of clarity; in reality, the secondary lines are more nearly parallel to the primary lines.

ple cuts while retaining structural integrity and sustaining only mild pinching, which is limited to the vicinities of the cuts. Thus, the lifetimes of these multiline tethers can be orders of magnitude longer than those of single-line tethers with comparable masses.

This work was done by Robert P. Hoyt and Robert L. Forward of Tethers Unlimited, Inc., for **Marshall Space Flight Center**. *For further information, please contact the company via e-mail at TU@tethers.com or visit their web site at http://www.tethers.com.*

Hoytether™ is a trademark of Tether Unlimited, Inc., for their interconnected multiline space tether design.

MFS-31305

Program for Computing Dynamics of Multiple Bodies

Relative to other programs used previously for the same purpose, computation times are reduced.

Lyndon B. Johnson Space Center, Houston, Texas

Symbolic Generator-Based Efficient Multibody Dynamics Algorithm (SOMBAT) is a program that enables speedy and accurate computations that solve equations of motion of multiple bodies. Originally intended for space-based applications (i.e., solving equations for the dynamics of a cluster of flexible bodies in orbit in real time), SOMBAT can also be applied in designing drugs, enhancing and otherwise processing images, the automotive industry, and robotics. It can also be used by the Department of Defense. Its greatest strength is its ability to reduce computation time without sacrificing accuracy. Unlike programs modeled on n^3 algorithms, SOMBAT accrues time savings overruns while satisfying short-turnaround requirements. Moreover, and vitally for the U.S. Space Program, the open and expandable format of SOMBAT will enable the tailoring of this program to upgrade add-on systems for new International Space Station (ISS) modules.

SOMBAT satisfies the specific need of NASA's International Space Station Program (ISSP) need for a software tool to simulate the dynamics of multiple bodies with large articulating angles in orbit. Before the advent of SOMBAT, simulation software tools followed an *order-of-n^3* approach. One pre-SOMBAT software tool, TREETOPS (a generic configuration-independent program with an n^3 algorithm) assembles equations of motion for all bodies in a configuration before solving for the dynamics at each time step. Because the size of the mass matrix (which size is an indicator of efficiency of computation) in TREETOPS is equal to the sum of all active degrees of freedom, TREETOPS becomes prohibitively slow when the number of active coordinates increases. Clearly, TREETOPS cannot be used to perform real-time simulations for ISS applications. Once it was determined that the generic nature of such simulation software as TREETOPS was not suited to the ISSP, another solution was sought.

SOMBAT is that solution. SOMBAT uses the ISS configuration to develop a more efficient algorithm that acts as a "smart" program to optimize generated code for the configuration. Savings are realized through two innovations: (1) improved mathematics for solving equations and (2) software that implements the improved

mathematics to optimize the simulation and avoid redundant calculations. The first innovation involves an order-of-*n* algorithm capable of exploiting the core-body/branch-body configuration to reduce all equations in terms of core-body degrees of freedom. Inasmuch as the inverted mass matrix generated by this algorithm is much smaller, the algorithm affords a substantial reduction in computation time.

The second innovation is a code-generator software tool — Codegen — that is able to develop a simulation based on active degrees of freedom. It does this by selecting equations of motion for a configuration without generating equations associated with degrees of freedom. Multiplication by zero is eliminated at the code-generation stage and the generated simulation is configuration-specific. As long as the configuration does not change, the same code can be used over and over again — a significant advancement. Codegen also simplifies equations by use of established mathematical relations, dot products, cross products, and linear algebraic relations; and it can take input from the user to optimize generated code. Together, these innovations ensure that SOMBAT achieves efficiencies unmatched by n^3 algorithms.

The major advantage of using SOMBAT is the recurring savings in computation time it delivers. In some ISS tests, SOMBAT was found to be 80 times faster than such older programs as TREETOPS. Although the generated code is configuration-specific (if the configuration changes, the code must be regenerated), this is not a major problem for SOMBAT, because SOMBAT easily regenerates code within minutes. Inasmuch as it accrues a saving of time over each run, SOMBAT is ideally suited to test runs. Moreover, its open and expandable format makes SOMBAT tailorable for future updates to the space-shuttle or Russian control systems on the ISS — systems that may be added to the ISS in the form of new modules. Finally, SOMBAT meets or exceeds industrial standards when it is applied in the other technological disciplines mentioned above. When speed and accuracy are needed to simulate the dynamics of multiple bodies, SOMBAT is faster and more accurate than any other algorithm currently available.

This work was done by Ramen Singh of Dynacs Engineering Company, Inc., for **Johnson Space Center**.
MSC-22782

Program Simulates Flights of Advanced Aerospace Vehicles

This modular software can be modified for analyzing different vehicles.

Marshall Space Flight Center, Alabama

Marshall Aerospace Vehicle Representation in C (MAVERIC) is a C-language computer program developed for use in performing high-fidelity simulations of flights and analyses of the guidance and control performances of the X-33 aerospace vehicle and the VentureStar reusable launch vehicle (RLV). A secondary purpose served by MAVERIC is determining indicators of vehicle parameters on realistic flight trajectories.

MAVERIC is in a state of continuing development. It is modular and is designed to be readily modifiable for simulating flights of other conceptual advanced aerospace vehicles; indeed, it has already been modified for use in simulating the flight of an orbital transfer vehicle.

The C computing language was chosen for MAVERIC because the X-33 flight software will be in C. Previous available programs that could have been chosen for the present applications were written in Fortran. These programs were not modular and not easily modifiable for high-fidelity computational modeling of the flight of the X-33.

MAVERIC includes subsystem models for the X-33 and the RLV, plus algorithms for monitoring guidance and control performance and trajectory-reshaping algorithms used to fly X-33 and RLV. A MAVERIC simulation can be started at a point other than liftoff. A simulation can include for all phases of flight from launch to the terminal-area energy-management interface [the interface between (1) re-entry into the atmosphere and (2) gliding flight through the atmosphere toward a landing point].

MAVERIC provides options for mathematical modeling of effects of winds, atmospheres, and dispersion. The Global Reference Atmosphere Model and range reference atmospheres are included. A Monte Carlo capability is provided for use in modeling dispersion. Dispersions that can be modeled include those of atmospheres, winds, propulsion, navigation, aerodynamics, and mass properties. Engine-out termination of flight can also be modeled.

MAVERIC is based on the Tframes modular software developed for the U.S. Army for use in simulating vehicles. Detailed descriptions and documentation for MAVERIC do not yet exist.

This work was done by James McCarter, Don Krupp, and Travis Dawson of **Marshall Space Flight Center**. *For further information, contact Larry Gagliano, MSFC Software Release Authority, at (256) 544-7175 or larry.gagliano@msfc.nasa.gov.*
MFS-31338

Books and Reports

Spacecraft Solar-Wind Trim Panels for Pointing

A report proposes that spacecraft assigned to orbits distant from the Earth be equipped with trim panels that would intercept the solar wind to generate small torques to correct for disturbance torques and thereby help to maintain the spacecraft pointed in the required directions. Paired panels would be placed on the ends of opposing moment arms equidistant from the center of mass of a spacecraft. The angles of the panels would be adjusted by use of servoactuators to control the solar-wind forces on the panels and thereby control the solar-wind-generated torques. This proposal would not only make it unnecessary to carry and consume a load of propellant to correct for disturbance torques; it would make constructive use of one of the primary causes of disturbance torques — the solar wind. The other disturbance torques that would also be compensated include those caused by solar-radiation pressure, gravity gradients, movements of mechanisms, movements of propellant fluids, and dumping of angular momentum through slowing down of reaction wheels.

This work was done by Richard K. Barry, Jr., of **Goddard Space Flight Center**. *To obtain a copy of the report, "Spacecraft Solar Wind Trim Panels for Pointing and Disturbance Torque Abatement" see TSP's [page 1].*
GSC-14247

BLANK PAGE

Machinery

Hardware, Techniques, and Processes

43 Four-Message Electromechanical Display System

42

BLANK PAGE

Four-Message Electromechanical Display System

The conventional limit of three messages could be overcome.

Marshall Space Flight Center, Alabama

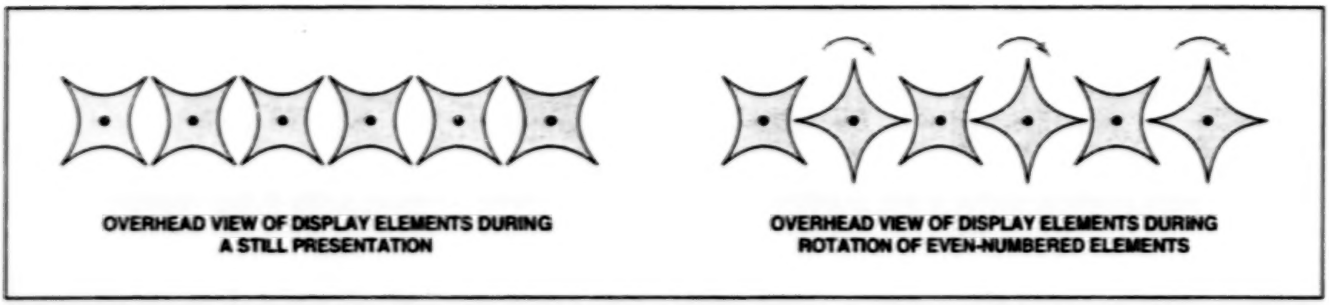
OVERHEAD VIEW OF DISPLAY ELEMENTS DURING A STILL PRESENTATION
OVERHEAD VIEW OF DISPLAY ELEMENTS DURING ROTATION OF EVEN-NUMBERED ELEMENTS

Each Display Element Would Have Four Faces, each showing part of a different message. The concavity of the faces is what makes it possible to use four faces (instead of the conventional three) in an unbroken display field: If the faces were flat, then it would be necessary to mount the display elements with gaps between them to prevent interference during rotation.

A proposed electromechanical display system would be capable of presenting as many as four different messages. Conventional electromechanical display systems are limited to three messages.

The three-message limit arises as follows: A typical electromechanical display system contains display elements with multiple flat faces that are rotated into view to present a message. Each display element could show, for example, a letter or number or part of an image. If the display elements have flat faces, then the number of messages is limited to three because three is the maximum number of sides of a polygon that can be placed contiguously with other, identical polygons along a common base line and that can be rotated without interfering with an adjacent polygon.

In the proposed system, each display element would have four concave cylindrical faces shaped so that the elements could be positioned contiguously on a display plane, yet could be rotated without mechanical interference with adjacent elements (see figure). Because of the curvature of the faces, messages could be partially visible at greater (in comparison with flat faces) angles off the perpendicular to the display plane.

There is one "catch": To prevent mechanical interference while a display element is being rotated, an adjacent display element must either remain stationary or else be rotated in the opposite direction with a 45° lag. This "catch" can be turned to advantage in that one can select from a variety of allowable sequences to draw attention to the display. For example, display elements could be rotated one at a time in any sequence, or the odd-numbered elements could be rotated while the even-numbered ones were held stationary, and vice versa.

This work was done by Richard T. Howard of **Marshall Space Flight Center**.

This invention is owned by NASA, and a patent application has been filed. For further information, contact Sammy Nabors, MSFC Commercialization Assistance Lead, at (256) 544-5226 or sammy.nabors@msfc.nasa.gov. Refer to MFS-31368.

BLANK PAGE

Mathematics and Information Sciences

Hardware, Techniques, and Processes

47 Program for Parallel Distributed Processing
47 Subpixel Map Registration and Estimation of Uncertainty
48 Software Interface Between MATLAB and a PC RS-232 Serial Port
48 Rapid-Prototyping Virtual-Reality Software Tool Kit
49 Software for Testing Access List Integrity

BLANK PAGE

Program for Parallel Distributed Processing

This software package automatically distributes mutually independent tasks to networked workstations.

Lyndon B. Johnson Space Center, Houston, Texas

A software system has been devised to manage automatically (1) the distribution of mutually independent computing tasks to computer workstations in NASA's Flight Design and Analysis System (FADS) network and (2) the execution of those tasks on those workstations. This program parallelizes serial tasks, making it possible to execute them concurrently. This program is a substantial improvement over previously developed special-purpose parallel-processing software systems used by NASA.

Parallel execution of tasks takes less time than traditional serial execution does. In the original FADS application, in which the tasks are principally simulations of spacecraft trajectories, this program significantly decreases the run time for simulating spacecraft missions. In a representative case of simulating 6 trajectories in the FADS, this software system can reduce the run time by 80 percent below the serial-processing run time.

This program can be modified to run on industry-standard workstation networks and is enhanced to handle many modes of operation. As workstation networks increasingly supplant large central computers, this program could become useful in increasing numbers of industrial applications.

Previously developed parallel-processing software concentrates primarily on how busy the computing resources (in this case, workstations) are when queried. The present software limits the distribution of tasks to workstations that are deemed to be idle in the sense that no users are logged into them and they are not executing other distributed work. This approach makes it possible for both distributed execution of tasks and logged-in users to coexist on the network platform without adversely affecting the users' performance.

This program includes three components: a Unix daemon program, a task-distribution executive, and a workstation executive. The daemon is a background program that is started during initialization of operation of each workstation in the network and is used by the distribution executive to determine the state (idle or busy) of each such workstation. The distribution executive reads a list of tasks to distribute, finds operational, idle workstations on the network, and uses the workstation executive to manage the execution of tasks on the available workstations. The distribution executive, keeping track of the status of each task, monitors the network for messages from the workstation executive. The workstation executive starts a task on an idle workstation and monitors both the task and the workstation. When a user logs into the workstation from its keyboard, the workstation executive removes the task from that workstation and notifies the distribution executive to resubmit the task to another idle workstation. When a task is completed, the workstation executive informs the distribution executive.

To maximize adaptability, simplify the development of algorithms, and reduce the cost of maintenance, the distribution and workstation-executive subprograms are written in Practical Extraction and Reporting Language (PERL), which is a very-high-level language (VHLL). In the original FADS application, this program works with the previously developed trajectory-simulating software, without need for any special modifications. However, for other applications, modifications can be made to make this program compatible with industry-standard workstation networks.

This work was done by Mark C. Allman of Rockwell Space Operations Company for **Johnson Space Center**. *MSC-22689*

Subpixel Map Registration and Estimation of Uncertainty

A normal distribution is fitted to the peak of a likelihood function in a pose space.

NASA's Jet Propulsion Laboratory, Pasadena, California

A method of determining the location and the uncertainty in the location of a mobile robot to subpixel resolution on a map grid has been devised. The method is applicable to a robot equipped with stereoscopic vision equipment for mapping the local terrain and with sensors for determining its orientation. The method involves fitting a parameterized surface (usually a normal distribution) to the peak of a likelihood function in the space of possible positions.

This method is built upon the method described in "Localization by Maximum-Likelihood Matching of Range Maps" (NPO-20392) *NASA Tech Briefs*, Vol. 22, No. 10 (October 1998), page 86. The localization problem is formulated as one of seeking a maximum-likelihood match of two maps: (1) a local range map generated by processing of images of the terrain in the immediate vicinity acquired by stereoscopic video cameras mounted on the platform and (2) a previously generated map of a larger surrounding terrain area (a "global" map). The global map could have been generated either by use of panoramic imagery from the robot or by combining the information from previously generated local maps. The points on the local range map are binned in a three-dimensional occupancy-grid representation of the surroundings, at a known orientation with respect to the global-map coordinates. In a subprocess that amounts to high-pass filtering of vertical-position data, the local average of the heights in each bin is subtracted from each cell. This subprocess reduces the computation time needed for localization by eliminating the need to search over vertical translations; in other words, as a result of this subprocess, it suffices to search over horizontal coordinates only.

The degree of matching between the global map and the local occupancy map is quantified by use of a likelihood function defined by the equation

$$L(X) = \prod_{i=1}^{n} p\left(D_i^X\right)$$

where D_i is the distance from the ith occupied cell in the local map to the closest occupied cell in the global map, X is the trial position of the robot (expressed as the trial position of the local map) relative to the global map, $p(D_i^X)$ is a probability distribution function (PDF), and n is the number of occupied cells. The most likely position of the local map relative to the global map [that is, the position, X, that maximizes $L(X)$] is taken to be the position of the robot. The

search for this position is started on a relatively coarse grid, from a position that has been estimated, for example, by deductive reckoning. The estimate of position is then refined in a subprocess that involves recursive division of the search space into smaller cells and pruning of cells that cannot pass the maximum-likelihood test.

As described thus far, this method is nearly identical to the method described in the noted prior article. The distinct aspect of this method lies in the provision for both subpixel localization and characterization of uncertainty in the localization. Inasmuch as the likelihood function expresses the probability that each position in the pose space (the space of possible positions) is the actual robot position, the uncertainty in the localization is quantified by the magnitude of the decrease of the likelihood function with distance from the peak. Subpixel localization in the discretized pose space can be performed by fitting a parameterized surface to the peak that occurs at the most likely robot position.

For the purpose of this fitting, it is assumed that in the vicinity of its peak, the likelihood function can be approximated and parameterized as a normal distribution. The fitting then yields both the subpixel estimate of position (namely, the center of the normal distribution) and an estimate of uncertainty (namely, the standard deviation of the normal distribution) centered at the nominal peak location.

The uncertainty is further characterized by a probability that a qualitative failure has occurred. Such a failure could occur, for example, in an environment in which recognizable landmarks are sparse and consequently many locations appear very similar to the robot. The probability of qualitative failure is estimated by comparing the likelihood scores under the tallest peak with the likelihood scores in the rest of the pose space.

This work was done by Clark F. Olson of Caltech for **NASA's Jet Propulsion Laboratory**. *Further information is contained in a TSP [see page 1].*
NPO-20657

Software Interface Between MATLAB and a PC RS-232 Serial Port

This software provides a relatively well behaved communication interface.

Marshall Space Flight Center, Alabama

A computer program establishes an interface between the MATLAB software and the serial data port of a personal computer (PC) that runs either the Windows 95 or the Windows NT operating system. The program makes it possible to utilize the graphical user interface (GUI) and the data-acquisition, control, and data-analysis capabilities of MATLAB while sending or receiving data via the RS-232 serial port. The data in question can be exchanged with external serial-communicating electronic circuitry, which could include another personal computer.

From the MATLAB command line or GUI, the user can initialize a serial-port session, cause the PC to write a byte to (or receive a byte from) the port, then terminate the session. The program provides a single command, "SerIO('x')," that acts in one of five different ways, depending upon which of four allowable values of the parameter *x* is specified:

- "SerIO('i')" initializes a Windows 95 or NT serial-port communication interface.
- Once initialization has been accomplished, "byte=SerIO('r')" utilizes a Windows 95 or NT kernel to read a single byte from the serial port and returns the value of the byte in "byte."
- "SerIO('w',byte)" utilizes the kernel to write the byte parameters to the serial port.
- "SerIO('d')" destroys the Windows 95 or NT serial-port handle that was created by "SerIO('i')" and used for reading and/or writing.
- "SerIO('?')" can be used to ask whether initialization has been performed.

An important feature of this program that helps to distinguish it from programs developed previously for the same purpose arises from the use of the Windows 95/NT kernel calls instead of direct inputs to and outputs from the hardware address of the serial port. This feature is advantageous in that it provides for a better behaved communication interface.

The program utilizes the Microsoft Visual C/C++ compiler in conjunction with the external-file-development capabilities of MATLAB. The program implements 4,096-byte transmitting and receiving buffers that enable communication between systems with varying transmission speeds. The program can readily be modified to return a vector of data (in contradistinction to a single byte) to the MATLAB software environment in order to accelerate or off-load MATLAB processing.

This work was done by Brandon Dewberry of **Marshall Space Flight Center**. *For further information, contact Larry Gagliano, MSFC Software Release Authority, at (256) 544-7175 or larry.gagliano@msfc.nasa.gov.*
MFS-31391

Rapid-Prototyping Virtual-Reality Software Tool Kit

The user need not engage in a tedious learning process.

Lyndon B. Johnson Space Center, Houston, Texas

The VrTool computer program enables its user to rapidly develop a prototype virtual-reality (VR) application program. Users of VR application programs need software that can help them keep pace with the rapidly evolving VR field. None of the previously commercially available VR software tool kits affords rapid-prototyping capabilities because all require users to generate their own code. This makes it necessary for users to engage in a tedious learning process to gain understanding of the application-program-generation process, which is also tedious.

VrTool offers a high-level user interface that makes it unnecessary for its user to engage in a tedious learning process; only minimal amount of learning time is necessary, and so the user can begin creating a VR environment almost immediately. As far as is known, no previously commercially available VR program offers a user interface that gives the user such a capability. The VrTool software would benefit any industry in which VR applications are used for simulations; examples of such industries include the aerospace, education, and medical industries.

VrTool includes four components: (1) a controller, which controls all other VR

processes; (2) a renderer, which displays graphical information; (3) a collision-detection processor, which determines whether there are collisions among objects; and (4) a user-interface subprogram, which builds the VR scene. VrTool was developed for Silicon Graphics workstations and includes drivers for VR peripherals.

This work was done by J. Mark Voss of the Lincom Corporation for **Johnson Space Center**.
MSC-22693

Software for Testing Access List Integrity

Many networks rely on firewalls or filtering routers for frontline network security. Packet filtering firewalls or routers filter incoming or outgoing packets based on a set of access rules. The IP (Internet Protocol) Packet Generator computer program assists in verifying that a packet filtering firewall is configured correctly, by detecting security holes in the firewall's filtering rules. The IP Packet Generator enables the user to build TCP/IP (Transmission Control Protocol/Internet Protocol) packets and transmit them via the network, to detect errors in access list configuration. The user can specify the source IP address of a packet to simulate attempted access from a remote host. The user can also specify the destination IP address, the type of packet, the destination port number, the size of the packet, the number of packets to send, and the packet rate. Thus, the software helps the user perform an exhaustive test of the access list.

This work was done by Becky Johnson, Mark T. Page, and Henry W. Yu formerly of I-NET for **Kennedy Space Center**.

Inquiries concerning rights for the commercial use of this invention should be addressed to the Technology Programs and Commercialization Office, Kennedy Space Center, (407) 867-6373. Refer to KSC-11878.

BLANK PAGE

Life Sciences

Hardware, Techniques, and Processes

53 Determining Glucose Levels From NIR Raman Spectra of Eyes

53 Improved Electrical-Impedance Body-Fluids Monitor

BLANK PAGE

Determining Glucose Levels From NIR Raman Spectra of Eyes

Spectra are processed by principal-component analysis, then artificial neural networks to obtain Bayesian probabilities.

NASA's Jet Propulsion Laboratory, Pasadena, California

A developmental noninvasive method of determining the concentration of glucose in blood is based on (1) the acquisition of a near-infrared (NIR) Raman spectrum from the aqueous humor of an eye, (2) analyzing the spectrum by a combination of techniques described below, and (3) recognition that the glucose level in the aqueous humor of the eye is about 80 percent of that in the blood 30 minutes before the spectrum was acquired. More specifically, what the analysis yields is a probabilistic indication that the glucose concentration represented by the Raman spectrum lies in one of three ranges of physiological interest: hypoglycemic (<3.9 mM), normal (3.9 to 5.8 mM), or hyperglycemic (>5.8 mM). The method involves less NIR laser power and shorter data-collection times than have been used in previous efforts to use Raman scattering to measure glucose concentrations in blood.

One reason for choosing the aqueous humor of the eye as the target for Raman spectroscopy is, of course, that the interior of the eye is optically accessible. Another reason is that whole blood contains numerous optically active materials, the spectra of which obscure the spectral signature of glucose. In comparison with whole blood, the aqueous humor of the eye contains many fewer Raman-active substances to complicate the overall Raman spectrum and the interpretation thereof.

The Raman-active substances in the aqueous humor of the eye are glucose, ascorbate, lactate, urea, and small amounts of protein. The Raman spectrum (absorbance vs. wavelength) of each of these is affected by interactions with all of the other substances present in the aqueous medium, resulting in both linear and nonlinear variations in Raman spectra with concentrations. Thus, even though only four or five Raman-active constituents are present in significant concentrations, it is necessary to use both linear and nonlinear multifactor analytical techniques to obtain accurate estimates of glucose concentrations from the total Raman spectrum.

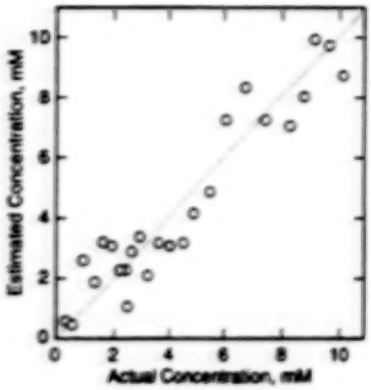

Concentrations of 24 Glucose Solutions as estimated from Raman spectra by the method described in the text agreed fairly well with the actual concentrations. In this case, the concentrations estimated by a neural network correspond to a nonlinear least-squares fit to the actual concentrations, with a regression coefficient of 0.955.

In the present method, sets of measured total Raman spectra are first subjected to the classical multivariate-analysis technique known as principal-component analysis. This technique yields a reconstruction of input spectra as linear combinations of feature vectors (eigenvectors of a covariance matrix) that account for the maximum variance in the input spectra. This reconstruction is optimum in the least-squares sense and involves the fewest parameters.

Each feature vector is fed as input to an artificial neural network that is configured to generate either one output or three outputs indicative of the corresponding glucose concentration. Prior to use in this way, the neural network must be trained by use of feature vectors representing known concentrations. Thereafter, if the neural network is configured for one output, then when it is presented with a feature vector from an unknown concentration, the output signal level should represent an estimate of the concentration; alternatively, if the neural network is configured for three outputs, then the signal level at each output terminal should represent a Bayesian *a posteriori* probability that the glucose concentration lies in one of the three ranges of physiological interest.

In vitro experiments on aqueous solutions of glucose at concentrations from 1.01 to 10.1 mM have demonstrated the feasibility of the method. In these experiments, specimens were illuminated with 100 mW of power at a wavelength of 785 nm from a cavity-stabilized laser diode. The Raman spectrum excited by this illumination was measured by use of a holographic imaging spectrographic probe head containing a liquid-nitrogen-cooled charge-coupled device (CCD). The output of the CCD was digitized and processed as described above, using commercial data-acquisition, multifactor-analysis, and neural-network software. The figure depicts some results obtained with a single-output neural network.

This work was done by Michael Storrie-Lombardi, James Lambert, and Mark Borchert of Caltech for **NASA's Jet Propulsion Laboratory**. *Further information is contained in a TSP [see page 1].*
NPO-20414

Improved Electrical-Impedance Body-Fluids Monitor

Measurements that yield a variety of data can be done quickly, frequently, and safely.

Lyndon B. Johnson Space Center, Houston, Texas

The Johnson Space Center (JSC) body-fluids monitor advances the state of the art of measuring hydration levels in humans during spaceflight. Neither bulky nor heavy, this noninvasive instrument is built around a commercial inductance-capacitance-resistance meter, which is used to obtain electrical-impedance-vs.-frequency data for equivalent-circuit/electrical-components analyses. The instrument is expected to prove invaluable not only in spaceflight settings but also in such other settings as veterans' hospitals, clinical facilities, and medical research laboratories.

The nearest commercial competitor is an instrument, based on a resistance-capacitance meter, that is used to perform bioelectrical response spectroscopy (BERS) for determining hydration levels. Going beyond the commercial instrument, the JSC body-fluids monitor also rates cerebral and other regional blood flows and cardiac outputs by use of time-based assessments of resistance and/or

inductance, noninvasively gauges blood pressure by use of resistance and inductance alone, and estimates the lean and muscle mass of a subject's upper and lower limbs in terms of the values of resistors, capacitors, and/or inductors of equivalent circuits derived from electrical-impedance measurements of the human body. A major feature that distinguishes the JSC body-fluids monitor from the commercial instrument is the capability to obtain and utilize data on inductances in addition to resistances and capacitances. Moreover, unlike the commercial instrument, the JSC body-fluids monitor can discriminate between vascular and extravascular water.

Some other methods of measuring hydration levels involve the dilution of tracer substances in the subject's body: In the total-body-water (TBW) method, one uses deuterium-labeled water; in the extracellular-fluid-volume (ECF) method, sodium bromide; and the plasma-volume (PV) method, radioactive iodine attached to albumin. In another method, total body volume is calculated from hematocrit and PV, and bioelectric-impedance analysis (BIA) [which involves measurement of impedance at a single frequency] is used to estimate TBW and ECF. Many of these methods are invasive, and most are time-consuming (a typical measurement takes between 1 and 6 hours), and cannot be repeated until the diluted tracer substances leave the body. These methods also cannot provide information during on-orbit operations. Worse, BIA produces measurement errors greater than those of dilution techniques. Moreover, the performance of the resistance-capacitance-meter-based BERS commercial instrument mentioned above has been challenged because its design makes no provision for modeling inductances; this is critical because inductors are key to the modeling of total blood volume (TBV) and PV.

In 1928, K. Cole originated the concept of using alternating-current measurements to characterize dielectrics dispersed in a conducting medium. In 1941 K. Cole and R. Cole refined this concept into the Cole-Cole principle, which has been applied to biological problems since the early 1960s. For the purpose of Cole-Cole analysis, the human body is treated as both a cylinder and an insulator (cell membranes) surrounding small conductors (the intracellular fluid) embedded in a larger conductor (extracellular water).

Therefore, the human body is treated as a parallel circuit, one limb of which is a purely resistive element that represents extracellular fluid. The other limb, representative of the intracellular component, consists of a resistance and capacitance in series. The commercial instrument mentioned above, operating over the frequency spectrum from 5 Hz to 1 MHz, generates BERS data that are used to compute the resistances and the capacitance.

The JSC body-fluids monitor operates over the frequency spectrum from 5 to 300 kHz. It functions similarly to the commercial instrument except that, as noted above, its design and method of operation account for inductance in addition to resistance and capacitance. More specifically, an inductor is added to the resistance limb; thus, the equivalent-circuit model used to analyze the BERS data is one limb (consisting of a resistor in series with a capacitor) in parallel with another limb (consisting of a resistor in series with an inductor). The inductor represents the inductance of the blood vasculature.

The JSC body-fluids monitor differentiates between vascular and extravascular water even as it noninvasively provides data for an assessment of a subject's TBW, ECF, TBV, PV, and changes in TBV and PV (ΔTBV and ΔPV). These assessments can be performed quickly and safely, and can be repeated frequently. The JSC body-fluids monitor could also be used to estimate the percentage of body fat, given the assumption that the lean tissues of the body are normally hydrated.

For operation of the JSC body-fluids monitor, a subject is instrumented with four standard electrocardiogram electrodes. Two electrodes are placed on the hand (wrist and knuckles), and two are placed on the foot (ankle and base of toes). A small electric current (below the human ability to feel) is introduced, and the magnitude and phase angle of impedance are recorded as the frequency is varied from 5 to 300 kHz. Electrical-component analysis of the measurement data produces three values of resistance (representing TBW, ECF, and intercellular water content), self and mutual inductance, and capacitance. These electrical-component values, along with the height and weight of the subject, are inserted in computational models developed to assess TBW, ECF, TBV, PV, ΔTBV, and ΔPV. Thus, the JSC body-fluids monitor and the associated data-analysis method yield a greater assortment of data than does any similar instrument/method combination heretofore used to measure a subject's hydration levels.

This work was done by Steven F. Siconolfi of **Johnson Space Center**. *Further information is contained in a TSP [see page 1].*

This invention is owned by NASA, and a patent application has been filed. Inquiries concerning nonexclusive or exclusive license for its commercial development should be addressed to the Patent Counsel, Johnson Space Center, (281) 483-0837. Refer to MSC-22491.

END

12-4-01